

UAS BASED PHOTOGRAMMETRY: A NEW TOOL FOR MONITORING BEACH
NOURISHMENT PROJECTS: A GALVESTON, TX TEST CASE

A Thesis

by

BENJAMIN MILLER RITT

Submitted to the Office of Graduate and Professional Studies of
Texas A&M University
in partial fulfillment of the requirements for the degree of
MASTER OF MARINE RESOURCES MANAGEMENT

Chair of Committee,	Glenn A. Jones
Committee Members,	Wesley Highfield
	Jens Figlus

Head of Department,	Kyeong Park
---------------------	-------------

December 2018

Major Subject: Marine Resources Management

Copyright 2018 Benjamin Miller Ritt

ABSTRACT

In December of 2016 the “Phase III Beach Nourishment: Seawall East” project started laying down approximately 920,000 m³ of sand dredged from the Big Reef area on the East end of Galveston Island, TX across 6.2 km of Seawall beaches from 10th Street to 61st Street. This project offered a unique opportunity to collect data on a pre-nourished beach area and monitor that same area monthly post-nourishment over the course of a year. Information on the health and life span of beach nourishment projects is valuable to coastal managing agencies, who require detailed data to back up the investment they have made, as well as for planning future projects. A low cost, easy to use, and quick survey method is required so that such agencies can better monitor their beaches for these purposes. For this thesis a deployment protocol was developed for Unmanned Aircraft System (UAS) based photogrammetric modeling methods which were used to generate photorealistic LiDAR quality point clouds to create profiles and sand volume calculations of this beach area for 14 months. Analysis of the data from this survey was conducted to monitor sand retention of the nourishment and documented 26.2% volume loss per year. Wave height data gathered from a NOAA oceanographic and weather buoy near Galveston was compared to beach volume and profile changes which indicates that wave energy as well as high impact tropical storms had a degree of influence (i.e. 24,505 m³ lost due to Hurricane Harvey) on the newly nourished beach.

ACKNOWLEDGEMENTS

I would like to thank my committee chair Dr. Jones as well as Dr. Figlus and Dr. Highfield for their guidance and support throughout the course of this research.

Thanks also go to my friends and colleagues and the department faculty and staff for making my time at Texas A&M University at Galveston a great experience.

I would like to thank my French Press and the wonderful coffee it made, without which I could not have pulled all night processing and writing marathons.

Finally, thanks to my mother and father for their encouragement, their patience, and love.

CONTRIBUTORS AND FUNDING SOURCES

This work was supervised by a thesis committee consisting of Professor Dr. Glenn A. Jones of the Marine Sciences Department and Professor Dr. Wesley Highfield of the Marine Sciences Department, and Professor Dr. Jens Figlus of the Department of Ocean Engineering. All work for the thesis was completed independently by the student.

Funds to purchase equipment used to collect and process data were provided by The Texas Sea Grant College Program's Grants-In-Aid of Graduate Research Program and the Texas Comprehensive Research Fund. Funds were used to Purchase the DJI Phantom 4 Pro and Matrice 600 UAS', peripheral UAS equipment, and data analysis software.

NOMENCLATURE

DEM	Digital Elevation Model
DJI	Dà-Jiāng Innovations Science and Technology Co., Ltd
GPS	Global Positioning System
GCP	Ground Control Point
IMU	Inertial Measurement Unit
LiDAR	Light Detection and Ranging
NOAA	National Oceanographic and Atmospheric Administration
SfM	Structure from Motion
SWH	Significant Wave Height
UAS	Unmanned Aircraft System
UAV	Unmanned Aerial Vehicle

TABLE OF CONTENTS

	Page
ABSTRACT	ii
ACKNOWLEDGEMENTS	iii
CONTRIBUTORS AND FUNDING SOURCES.....	iv
NOMENCLATURE	v
TABLE OF CONTENTS	vi
LIST OF FIGURES	viii
LIST OF TABLES	x
1. INTRODUCTION & PREVIOUS LITERATURE.....	1
2. STUDY AREA AND DATA	4
3. METHODS	11
3.1 Introduction.....	11
3.2 UAS Deployment Methodology and Testing.....	12
3.3 Ground Control Point and Scale Bar Placement.....	14
3.4 UAS Data Processing and Analysis	17
3.5 Wave Height Data Processing and Analysis.....	23
3.6 Ground Truthing.....	27
4. RESULTS.....	29
4.1 Introduction.....	29
4.2 Volume Change and Nourishment Lifespan.....	29
4.3 Volume Change and Relationship to Significant Wave Height.....	32
4.4 Feature Recognition.....	35
5. DISCUSSION.....	36
6. CONCLUSION.....	39
REFERENCES	41
APPENDIX A	45
APPENDIX B	60

APPENDIX C	61
------------------	----

LIST OF FIGURES

	Page
Figure 1 USACE Galveston Sand Management Plan map with Reach 1 where the Phase III Nourishment occurred, reprinted from <i>Galveston Island, Texas, Sand Management Strategies</i> . (Technical Report No. ERDC/CHLTR-16-13) (Frey et al., 2016).....	6
Figure 2 Location of the study area on Galveston Island Texas (green) along with the other five beaches maintained by the city of Galveston (red dots) and the Big Reef sand source near East Beach used for the nourishment project (red polygon). Modified from (Google Earth, 2018).....	7
Figure 3 The 5 sections of Phase III Beach Nourishment: Seawall East study area. Modified from (Google Earth, 2018).....	8
Figure 4 The DroneDeploy flight plan used for Section 1. *Produced using DroneDeploy.	9
Figure 5 Location of the 2 beach segments excluded from data analysis created using google earth. Modified from (Google Earth, 2018).....	12
Figure 6 GCP placement along the seawall and groins of section 3. *Produced using Agisoft Photoscan Pro	15
Figure 7 Example of a 0.914 m scale bar with coded targets.	16
Figure 8 Section 1 Beach segment 1 dense point cloud with volume polygon and profile polyline. *Produced using Agisoft Photoscan Pro	18
Figure 9 December 2016 digital elevation model (DEM) of Section 1 Beach segment 1 with volume polygon and profile polyline. *Produced using Agisoft Photoscan Pro.....	19
Figure 10 May 2017 DEM of Section 1, Beach segment 1 with volume polygon and profile polyline. *Produced using Agisoft Photoscan Pro	20
Figure 11 Volume calculation for Section 3, Beach segment 3 using mean sea level (MSL) as the baseline. *Produced using Agisoft Photoscan Pro	21
Figure 12 Profile measurement for Section 3, Beach segment 3. *Produced using Agisoft Photoscan Pro	21
Figure 13 Average beach profile change for the 14 months of the study.	22
Figure 14 Change in each beach volume and average beach volume for the 14 months of the study. Note The 2.2 km length of beach segments 13* & 14* are estimated volumes as they could not be measured due to overhanging structures.....	22

Figure 15 Histogram of SWH per hour for May 2017 through April 2018. Range 0.1-0.2 m to 3.5-3.6 m. Skewness 1.018.	24
Figure 16 Significant Wave Height and the number of hours they were prevalent. Note the large number of hours (93) with waves over 2.0 m during August 2017 (month of Harvey making landfall) vs the previous month of July 2017 in which no waves were over 1.4 m. The number of hours for waves less than 1.0 m are not shown. Despite making landfall 253 km Southwest of Galveston the storm still influenced SWH at the study area.	24
Figure 17 Components of beach nourishment projects designed to erode at different rates, reprinted from Beach nourishment profile equilibration: What to expect after sand is placed on a beach. (Willson et al., 2017).	26
Figure 18 Difference in altitude measurements taken by RTK and UAS along the profile line used for ground truth testing. Note: Measurements were made at 1 meter intervals along a single profile extending from the base of the Seawall (0 m) to the water line (60 m).	28
Figure 19 Rate of loss and lifespan prediction for the Phase III Beach Nourishment Project. Note: Percentage of fill lost thru May 2018 was 26.2%	30
Figure 20 Rate of loss and lifespan prediction (with & without hurricane) for the Phase III Beach Nourishment Project. Note: Percentage of fill lost thru May 2018 was 26.2%. Percentage of fill lost if back-striping tropical storm effects was 15.7%	31
Figure 21 Hourly significant wave height for the month of August 2017 when Hurricane Harvey occurred. Compare with the other months shown in figures 15 & 16.	33
Figure 22 Relationship between monthly SWH skewness and monthly fill volume loss rate. Note the insensitivity of loss rate for SWH skewness values less than 1.0. This constancy allows greater confidence in extrapolating cumulative loss rates to predict timing of.....	34
Figure 23 Example of an erosional cut in Section 2, Beach segment 2 July 2017. *Produced using Agisoft Photoscan Pro.....	35

LIST OF TABLES

	Page
Table 1. Monthly Average Volume Data and Significant Wave Height Skewness Coefficients. Note: Monthly volume measurements represent the difference in change between 2 months, except for May 2017, SWH is for the month recorded.....	27
Table 2. List of USACE GenCade model output alternatives for Galveston Island restoration for Reach 1 (yellow). Note: Measurements made by USACE are in Imperial Adapted from “Galveston Island, Texas, Sand Management Strategies.” by A. E. Frey, 2016, (Technical Report No. ERDC/CHLTR-16-13), 88. Coastal and Hydraulics Laboratory: U.S. Army Engineer Research and Development Center. Units.....	32

1. INTRODUCTION & PREVIOUS LITERATURE

Studies of shoreline accretion/erosion are fundamentally important for guiding a wide-range of coastal management policies (Frey, Morang, & King, 2016; Jones, Schlacher, Schoeman, Weston, & Withycombe, 2017; Luijendijk et al., 2018; Turner et al., 2016). Galveston Island, Texas has a number of engineered beaches and coastal features that are impacted through coastal processes and extreme weather events on an annual basis. In an effort to maintain and grow Galveston's economy through tourism draw and protect the city's coastline from storm surge, the Galveston Park Board and the City of Galveston, Texas have enacted beach nourishment projects across the city's beaches. Since 1995 Galveston has spent almost \$58 million (2017\$) placing 2.4 million m³ of sand over four different nourishment cycles/projects (Songy, 2017). This large resource and financial investment to complete these projects requires that detailed monitoring should take place to better understand how accretion/erosion impacts these new beaches over the months and years after they are built. Such studies, if conducted over the first year after fill placement, can help to better predict the longevity of a new beach. This early prediction can in turn give coastal managers a longer lead time to plan for securing the funding and sand resources, needed for the next nourishment cycle.

In December of 2016 the Galveston Park Board acquired \$19.1 million from a Coastal Erosion Planning Response Act (CEPRA) grant from the Texas General Land Office (TGLO) along with matching funds from the Federal Emergency Management Agency (FEMA) to begin work on the "Phase III Beach Nourishment: Seawall East" project. This project used approximately 920,000 m³ of beach-quality sand dredged from the Big Reef area on the East end of Galveston Island to widen 6.2 km of Seawall beaches from 10th to 61st Street to 91.4 m (Frey

et al., 2016; Songy, 2017; Texas General Land Office Coastal Resources Office, 2017). The placement of sand began at the end of December 2016 and was completed in May of 2017.

This project offered a unique opportunity to collect data on a pre-nourished beach area and monitor that same area post nourishment monthly over the course of a year. However, due to the size of the study area (6.2 km in length and 133 hectares in area) and the type of data that was desired to be collected, a novel method of data collection was needed.

Traditional methods of beach surveying using RTK GPS systems, total stations, and ground-based LiDAR have been routinely used in monitoring beaches and coastal areas (e.g. Cheng, Wang, Guo, 2016). However, these systems, as well as, aerial-based LiDAR and satellite imaging are oftentimes expensive, labor intensive, or time consuming and therefore not conducted on as frequent a basis as desired for the month-to-month study of beach nourishment projects. UAS-based programmatic techniques can produce LiDAR-like point clouds generating high resolution topography from low cost UAS (Baltsavias, 1999; Boon, Marinus Axel, Greenfield, & Tesfamichael, 2016; Cook, 2017; Hugenholtz et al., 2013; Matese et al., 2015; Nikolakopoulos, Kozarski, & Kogkas, 2017; Weiss & Baret, 2017; Whitehead & Hugenholtz, 2014).

Subaerial survey techniques, specifically programmatic based ones, have been well researched by a wide variety of disciplinary fields and employed successfully by land surveyors, engineers, and land managers for more than a decade (Boon, M. A., Greenfield, & Tesfamichael, 2016; Casella et al., 2014; Daponte, Vito, Mazzilli, Picariello, & Rapuano, 2017; Long et al., 2016; Nex, F. & Remondino, F., 2014; Nikolakopoulos, Soura, Koukouvelas, & Argyropoulos, 2017; Papakonstantinou, Topouzelis, & Pavlogeorgatos, 2016; Rusnák, Sládek, Kidová, & Lehotský, 2018; Scarelli et al., 2017; Watanabe & Kawahara, 2016; Whitehead & Hugenholtz,

2014). With the advent of dependable and cost effective UAS becoming more prevalent in data collection in survey and monitoring projects, subaerial photogrammetry from SfM software like Agisoft PhotoScan Pro can now be deployed to efficiently collect surface data at a fraction of the cost and man-hours found with other techniques (Colomina & Molina, 2014; Nex, F. & Remondino, F., 2014; Qin, Tian, & Reinartz, 2016; Siebert & Teizer, 2014; Tonkin, Midgley, Graham, & Labadz, 2014; Toth & Grzegorz, 2016; Westoby, Brasington, Glasser, Hambrey, & Reynolds, 2012; Whitehead & Hugenholtz, 2014; Yahyanejad & Rinner, 2015). This makes UAS based photogrammetry a powerful tool for monitoring the subaerial portions of beach nourishment projects.

UAS-based photogrammetric methods for surveying and studying beach nourishment projects offer a level of detail that more traditional methods lack at a cost value that ground and aerial based LiDAR and imaging cannot match. However, this requires that a standardized deployment protocol be developed for deriving accurate elevational measurements for UAS-based beach surveys. This thesis details the development of such a protocol and its practical application by deriving volume and profile measurements for a newly nourished beach in Galveston Texas. The primary research question addressed in this thesis was: Could UAS-based photogrammetric modeling techniques provide the high-quality data sets needed to create beach profiles and beach volume calculations at least as well as RTK GPS based data sets, and if so what would be the best methodology for utilizing the UAS to do so?

2. STUDY AREA AND DATA

Galveston Island is a 46.6 km long sandy barrier island along the upper Texas coast (Figure 1), located approximately 72.4 km South-Southeast of Houston and approximately 70 miles West-Southwest of the Texas-Louisiana border. The island varies from approximately 0.96 km to 4.8 km in width and is oriented East-Northeast to West-Southwest (Figure 1).

Net longshore sediment transport for Galveston Island is predominantly to the Southwest (King, 2007; Ravens & Sitanggang, 2007a). However, from the Galveston Seawall near 61st Street to the entrance of the Galveston Shipping Channel the transport is to the Northeast (King, 2007). To the west of 61st Street, the net sediment transport direction is Southwestward towards the San Luis Pass. The primary reason for this reversal is due to changes in wave refraction due to offshore bathymetry (King, 2007; Ravens & Sitanggang, 2007a). Throughout most of the study area, wave conditions lead to the gross transport being greater than the net transport (King 2007). Due to these sediment transport conditions central Galveston Island is experiencing long-term erosion with both ends of the island are accreting sediments in the Big Reef area and the San Luis Pass.

The “Phase III Beach Nourishment: Seawall East” study area is a beach system with a groin field on Galveston Island, Texas and is located along the City of Galveston’s Seawall Boulevard between 10th and 61st streets (Figure 1). This area has been designated as Reach 1 by the US Army Corps of Engineers (USACE) Galveston District in their 2016 Galveston Island, Texas, Sand Management Strategies report (Figure 2). The goal of this report was to assist the City of Galveston in developing a long-term strategy for sand management to mitigate erosion and reduce the long-term cost of beach maintenance (Frey et al., 2016).

Galveston Island beaches are highly engineered and as such have a drastic effect on sediment transport, sediment retention, and beach nourishment design. Seawalls in general and the Seawall on Galveston, in particular, have the effect of fixing the shoreline in place, exacerbating lateral transport and erosion to the point that subaerial beaches will eventually disappear (Dean, R. G., 1986; Dean, Robert G., 1991). For this reason, groin fields are often placed with seawalls to reduce this sediment transport and in the case of Galveston, slow sediment transport along this section of the Seawall to protect the toe of the Seawall from undercutting (USACE, 1992). Due to this increased capacity for sand retention and the presence of a seawall where wave scouring is more prevalent, projects need to be specially designed for the sections along the Galveston Seawall (Todd Davison, Nicholls, & Leatherman, 1992).

As part of the Galveston Island, Texas, Sand Management Strategies report the segment of shoreline reaching from just North East of the Galveston North Jetty on Bolivar Peninsula to the San Luis Pass was divided into sediment budget cells (Figure 1). These cells are separated by their gain/loss of sediment, frequency of dredging, and characteristics of sediment transport unique to each cell.

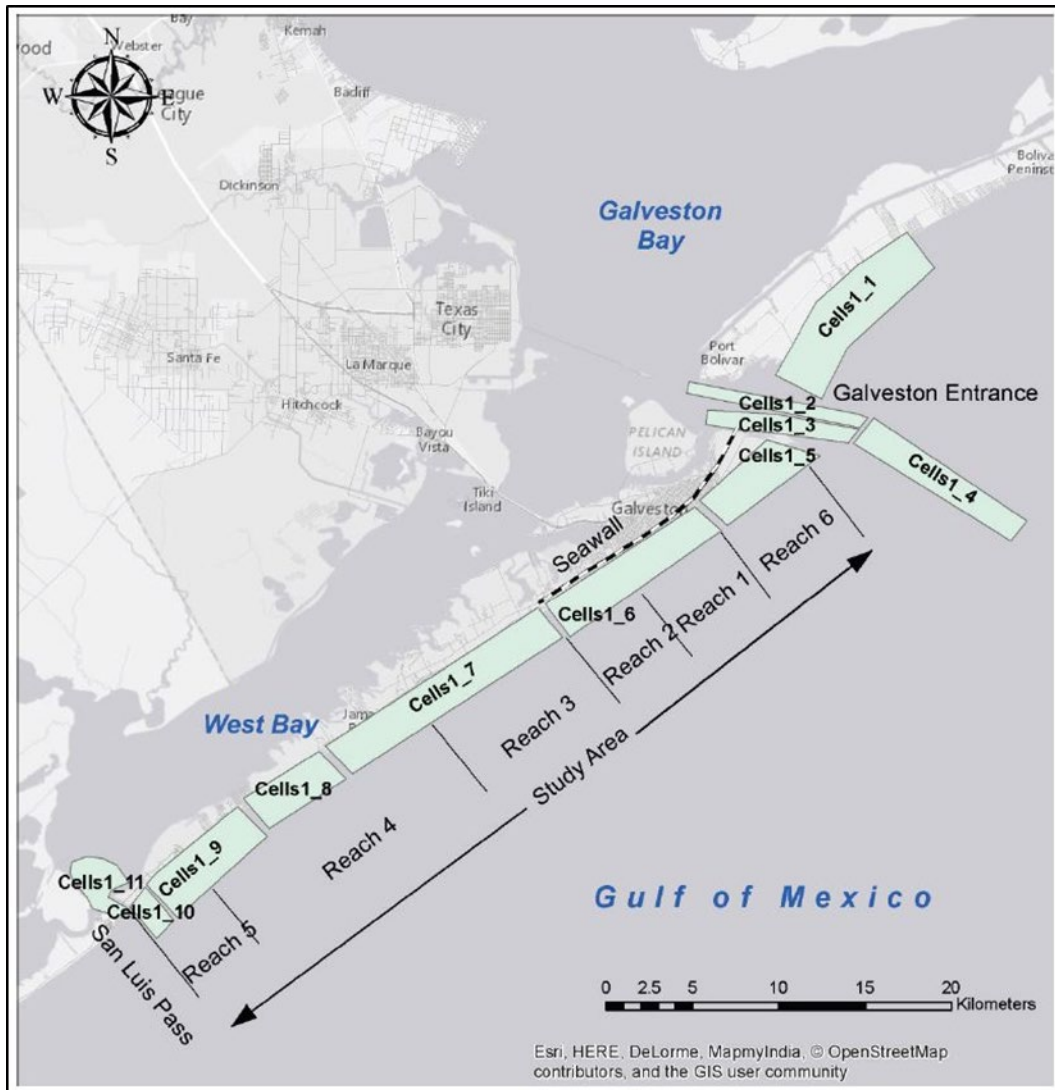


Figure 1 USACE Galveston Sand Management Plan map with Reach 1 where the Phase III Nourishment occurred. Reprinted from “Galveston Island, Texas, Sand Management Strategies.” by A. E. Frey, 2016, (Technical Report No. ERDC/CHLTR-16-13), 7. Coastal and Hydraulics Laboratory: U.S. Army Engineer Research and Development Center.

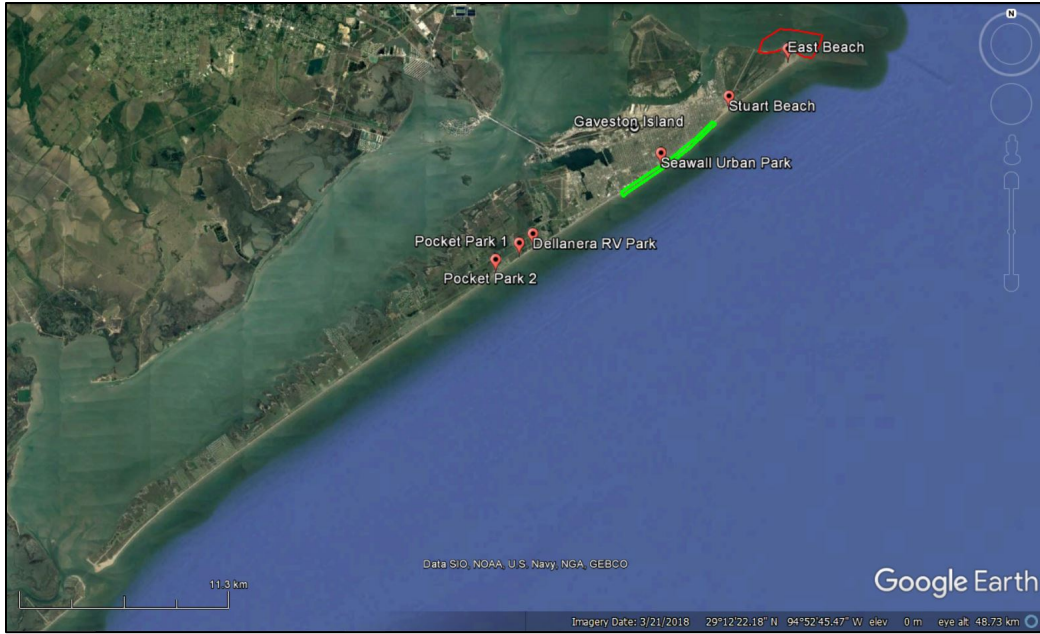


Figure 2 Location of the study area on Galveston Island Texas (green) along with the other five beaches maintained by the city of Galveston (red dots) and the Big Reef sand source near East Beach used for the nourishment project (red polygon). Modified from (Google Earth, 2018).

Reach 1 is 6.2 km in length and encompasses 133 hectares running along Galveston’s 16 km long 5.2 m high Seawall and contains a field of 15 groins breaking the area into 14 beaches segments. These beach segments comprise the Seawall Urban Park which is 1 of 6 beach properties maintained by the Galveston Park Board. These properties are a major tourist draw for the island, with the Seawall Urban Park being the longest of these beach parks (Figure 2).

In order to survey the Phase III Beach Nourishment: Seawall East over the course of 14 months using UAS, a series of flight plans needed to be developed in order to maintain constancy in flight altitude, overlap, and side-lap of the photos taken each month. The altitude, overlap, and side-lap ratio used for these flight plans created in the UAS control software package DroneDeploy was developed as part of this study and is detailed in the Methods section of this thesis and in the report “*Deployment Protocol Development for Deriving Accurate*

Elevational Measurements of a UAS-Based Beach Survey” found in **Appendix A**. Due to the size of the study area and flight time per battery limitation of the DJI Phantom 4 Pro UAS used in the study, the study area was divided into 5 sections in which each had its own flight plan (Figures 3 & 4).

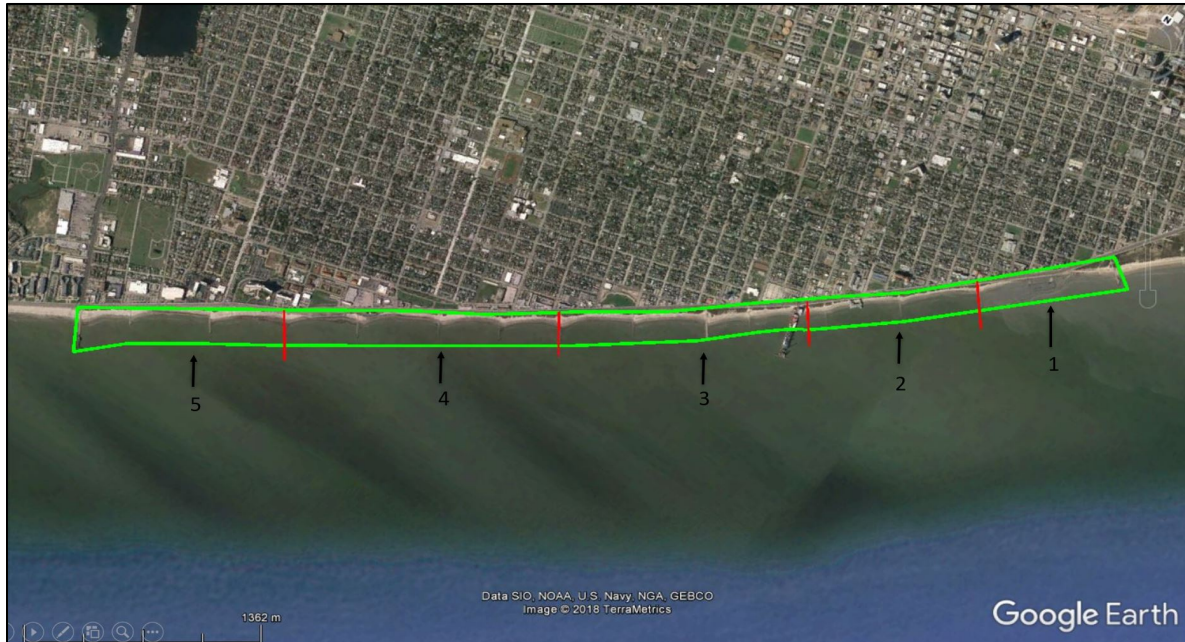


Figure 3 The 5 sections of Phase III Beach Nourishment: Seawall East study area. Modified from (Google Earth, 2018).

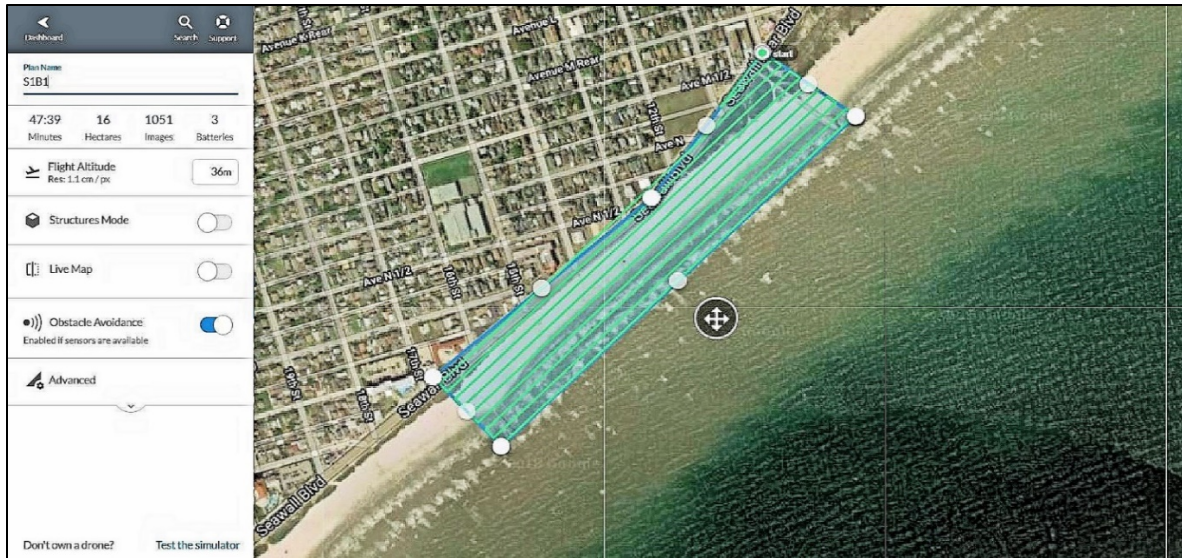


Figure 4 The DroneDeploy flight plan used for Section 1. *Produced using DroneDeploy.

Due to the nature of UAS-based photogrammetry, the photo sets for each of these sections would number between 788 to 1,648 individual photos depending on the section with 6,016 being taken of the entire 6.2 km study area each month. Over the course of 14 months 84,224 photos were taken and processed in Agisoft's photogrammetry suite Photoscan Pro to create LiDAR like point clouds, 3D meshes, Digital Elevation Models (DEMs), and orthomosaics used to study the nourishment project. In total 3.55 terabytes of data were collected and processed for this study.

Due to the study area's location on the Texas Gulf Coast, Hurricane Harvey (August 2017) was a factor to be considered when analyzing volume and profile change in the study area. Although Harvey made landfall 253 km to the southwest of Galveston, it nevertheless led to enhanced wave height and duration. In order to document the impact that this storm had on the study area as well as to better understand the overall forcing contributing to erosion, the significant wave height (SWH) data for the months of May 2017 through April 2018 was

analyzed using NOAA oceanographic and meteorological buoy LLNR 1200 located 35 km off Galveston at a water depth of 15 m.

As there are no near shore wave gauges along the Galveston Seawall, it was determined that studying the deep-water waves recorded at the offshore buoy would lend insight into the shallow water waves and breaking wave conditions at the study area shoreline. Knowing the high wind speeds associated with hurricanes are able to produce extreme waves and the increase in amplitude of the waves due to storm surge, certain assumptions about the relationship between deep-water waves and more impactful shallow/breaking waves could be made. The deep-water wave data from the NOAA buoy was processed using Microsoft Excel and its Data Analysis tool box to examine the relationship between wave height, sand volume loss, and beach profile change in the study area.

3. METHODS

3.1 Introduction

In order to accurately collect the UAS data and analyze it for comparison to the significant wave height (SWH) data a methodology had to be established for its deployment. Creating flight plans in Drone Deploy to gather consistent and accurate data and the choice in placement of each section's ground control points (GCPs) would be crucial to the processing and analysis of the UAS-based data in Agisoft Photoscan Pro, and for the analysis of gathered SWH data.

Two of these 14 beach segments were excluded due to overhanging structures (Murdoch's Souvenirs Shop at 22nd St in Section 2, and the Galveston Pleasure Pier at 25th St in Sections 2 & 3) (Figure 5). To avoid any injury to persons or property damage, no UAS flights were made in close proximity to the Galveston Pleasure Pier. While parts of the beach near these structures were imaged, the gap in imaging left by not flying over the Pleasure Pier or Murdoch's was not conducive to creating data of the quality desired for this study. In all, 2.2 km of the 6.2 km of nourished beach was excluded from the study leaving only 4 km of beaches (Figure 5).

An effort was made to estimate the volume of the fill that occurred for this section as well as what the total change in volume of the 2 beach segments in this 2.2 km area might be. This was done by measuring the distance between the groins of the 2 beach segments and comparing those to the rest of the groin field. Two beach segments from the groin field (Section 3 Beach segments 4 & 5) most closely matched the non-measured beach segments and volumes were extrapolated from these. These estimated volumes were modified to include the difference in volume due to the presence of pylons in the beach supporting the overhanging structures. To do

this 500 m³ of sand was subtracted from the estimated fills to be conservative. In total it is estimated that 106,405 m³ of sand was placed in this 2.2 km long section.

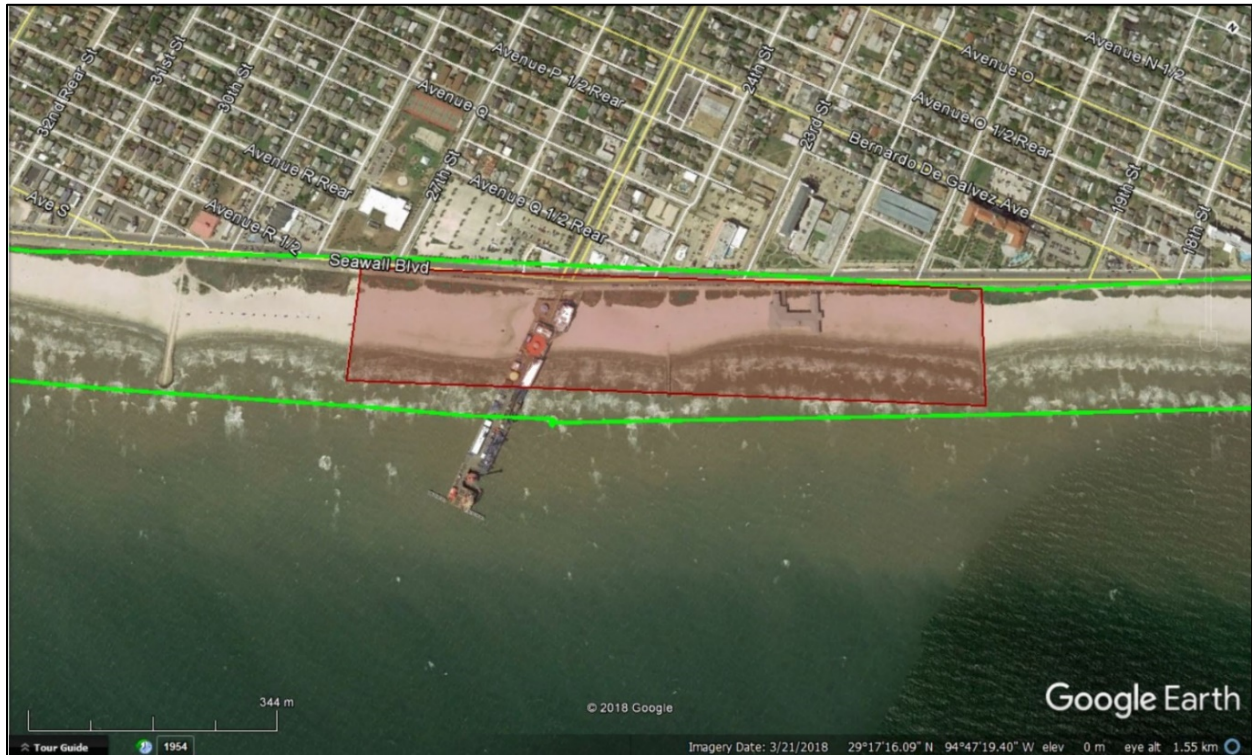


Figure 5 Location of the 2 beach segments excluded from data analysis created using google earth. Modified from (Google Earth, 2018).

3.2 UAS Deployment Methodology and Testing

There are many options in commercial-grade UAS platforms that can be used for photogrammetric surveys, with many of these types of systems providing accurate data through the use of onboard RTK systems, hi-resolution cameras, extended battery life, and advanced control software. As part of developing and testing the methodology we employed a commercial grade DJI Matrice 600 to compare with the performance of a consumer-grade DJI Phantom 4 Pro (see **Appendix A**). Commercial-grade systems exhibit better vertical resolution but are oftentimes cost prohibitive for researchers, managing agencies, and organizations looking to

gather fast, reliable information on coastal systems and projects. A solution to this issue is to use a consumer-grade UAS which can be employed as a less expensive option as long as quality assurance steps are taken to gather and create reliable data.

In order to assure the quality of data collected, a testing phase was conducted to ascertain the best methods using the consumer grade DJI Phantom 4 Pro UAS. This required a series of test flights to determine the number of Ground Control Points (GCPs), proper flight altitude, and to check the accuracy of measurements against those taken by the commercial-grade DJI Matrice 600 and ground-based RTK GPS.

The Phantom 4 Pro has a 20 Mega Pixel camera, onboard GPS, two IMUs, control hardware, and 20-30-minute battery life making it an excellent option for this kind of study.

Several factors had to be taken into consideration when determining when to deploy the UAS. Imaging the beach during the lowest possible tide was required so as to capture as much of the exposed beach as possible. This required that the low tide time frame for imaging also had to take place during a period of stable weather with wind gusts below 32 km per hour, no rain, and with the sun being at an altitude greater than 35° above the horizon. Proper lighting and angle of light are factors in photogrammetry that must be considered when completing the imaging phase. If the angle of light from the sun is such that it casts long dark shadows, the SfM software can interpret them as a change in depth or even negative space.

For 13 of the 14 months three consecutive days during the month was required to image the entire study area. For the 13 months where imaging went as planned flights took place between the 1st and 8th of each month. The exception was the month of March 2018. During this month wind gusts of 64 km per hour or higher were predicted for the optimal imaging time

frame. In order to still capture data for March a new low tide window, the 13th- 16th, was chosen when the high wind events had subsided.

The full development of the UAS deployment protocol used in the beach nourishment study and the lessons learned during this testing phase are detailed in the report “*Protocol Development for Deriving Accurate Elevational Measurements of a UAS-Based Beach Survey*” in **Appendix A**.

3.3 Ground Control Point and Scale Bar Placement

GCPs are essential for georeferencing the data sets and products produced in Agisoft Photoscan Pro. Their placement in the models allows for the accurate calculation of sand volumes and beach profiles using the elevation information they provide. During testing for the deployment protocol, a series of tests were conducted in which models were processed using different quantities of GCPs in an ascending order from 1, 5, 10, 20, & 40. Previous tests of the number and placement of GCPs across the area being surveyed indicated that the more, evenly placed GCPs provides a higher degree of accuracy in measurements (Boon, Marinus Axel et al., 2016). These tests indicated that errors in elevational accuracy decreased as the number of GCPs increased. The maximum error in elevation at any one of the check points was 3 cm when using 40 GCPs. Using the key elements learned in the development of the UAS deployment protocol described above, it was necessary to place at least 40 GCPs in each of the five sections that the beach was divided into (**Appendix A**).

Due to the size of the sections and the multiple features inside them individual sections were assessed for the need to add additional GCPs to provide the accuracy desired for high quality measurements needed for the study. For this reason, Section 1 with its two groins

only required 40 GCPs whereas the areas with 3 or more groins (Sections 2-5) were benefitted from more GCPs evenly placed across their surface, to ensure that the beach segments being surveyed had closely associated ground control. To this end Sections 2-5 had a total of 70 GCPs placed in them to provide adequate coverage. Due to uncontrollable variables such as tourists visiting the beach, beach maintenance personnel, and animals, it was decided to forgo the use of traditional target plates used for GCPs. It was observed that people and animals were often attracted to the target plates during the deployment protocol testing. Since any interference with the plate would invalidate the use of the GCP and the RTK GPS measurement taken at it, static features in the hard structure of the seawall and groin field were chosen to be used as reference points to create GCPs (Figure 6).



Figure 6 GCP placement along the seawall and groins of section 3. *Produced using Agisoft Photoscan Pro

This system of static GCPs also reduced the need to deploy the RTK GPS to measure GCPs for each monthly flight of the study reducing the time requirements and personnel in the field. In addition, this also allowed for a rapid response to any extreme weather events (i.e. Hurricane Harvey in August 2017).

Locations in the hard structure in each section common to each month of the study were measured once using the RTK GPS for use as GCPs, these included concrete benches built on top of the seawall, and drill marks on easily recognizable stone blocks in the groins.

Measurements using the RTK GPS were converted from northing, easting, and altitude measurements to WGS 1984 (EPSG:3426) to match the geoid used in Agisoft Photoscan Pro to create products and derive data.

In addition to GCPs, 2 scale bars were placed in a “T” pattern on the beach of each section when it was being imaged as a means of quality control. These scale bars measuring 0.914 m in length have a coded target plate at each end. These targets are generated by Agisoft Photoscan Pro and can be automatically detected by the software (Figure 7). At the end of the imaging of a section the UAS would be flown to the location of these scale bars and they would be imaged at a height of 36m then 20m then 5m. This process allowed these images to be aligned in Agisoft Photoscan Pro with the rest of the images taken for the section while ensuring that the coded targets would be clearly visible.



Figure 7 Example of a 0.914 m scale bar with coded targets.

Using the **Detect Marker** function of Agisoft Photoscan Pro the section is scanned for coded targets, automatically placing markers at the center of the detected targets. After each step of the processing phase after GCP placement, the distance between the markers on each scale bar were measured for quality control. Deviation from the known 0.914 m distance between target centers would indicate that GCPs are misplaced or that an error has occurred in the generation of the Dense Cloud or Mesh. This was essential for detecting any issue in processing that might affect the overall end product.

3.4 UAS Data Processing and Analysis

The images captured using the UAS were aligned, and dense point clouds, meshes, georeferencing, and production of DEMs, and orthomosaics were produced in Agisoft Photoscan Pro using the workflow detailed in **Appendix B**. This same software package contains a suite of tools that allows for analysis of the products it produces. These include a tool for measuring profiles based off drawn polylines and volumes using drawn polygons. These shapefiles were drawn on the dense clouds of each monthly iteration of the models so as to only measure the visible sand and not interpolate data beyond the scope of the know beach area (Figure 8).

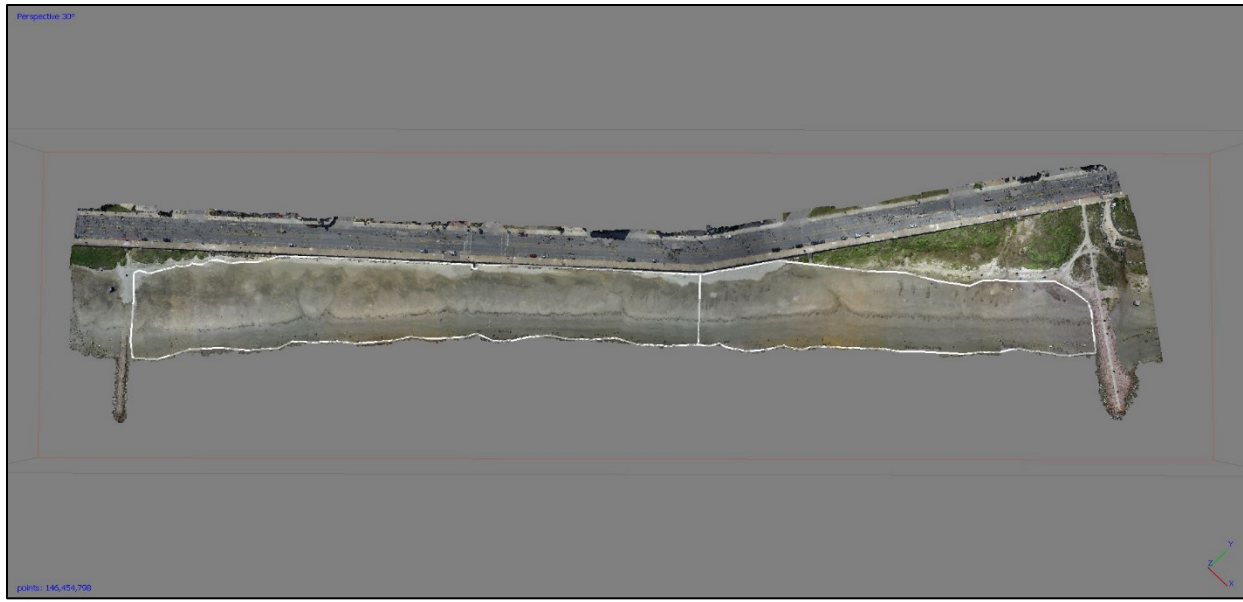


Figure 8 Section 1 Beach segment 1 dense point cloud with volume polygon and profile polyline. *Produced using Agisoft Photoscan Pro

It is important to note that in order to measure the volume of sand in each of the beach segments, and only the sand, steps had to be taken during processing to remove objects that were not part of the beach from the dense cloud before mesh creation. These included beach umbrellas, lifeguard stands, trucks, trashcans, and groups of people. Once the objects were clipped from the dense cloud, an interpolative function in the mesh creation function was used to fill the holes created using data points from around the hole. This process allowed for the measurement of a “clean beach”.

Comparing the DEMs created for the December 2016 pre-nourishment flights to the May 2017 post-nourishment flight the landward terminating line for the polygons was determined for the 12 beach segments in the five sections. This line was drawn at the foot of the seawall and/or along the toe of dunes as they applied to each beach. No vegetated dune structures were measured in this study due to the limiting factors of determining vegetation height and growth in

each model as well as the fact that these structures were avoided in the overall Phase III nourishment project. While some embryonic dune growth was seen in areas that acted as wind shadows along the Seawall, such as stair cases, actual measurements of dune growth would be required to determine how much beach material was being incorporated into or eroding from these features.

Once the shapefiles for the polygons and profile lines were created for the December 2016 pre-nourishment models, they were imported into the other 13 months of models to ensure that the dune and seawall lines were kept the same while the seaward lines would be adjusted to changes in the shoreline. Profile lines were also imported and extended to the edge of each dense point cloud at the waterline for each of the models to ensure that the same profile line was measured each time (Figures 9 & 10).

Once the shape files had been imported and resized to follow the change in shoreline, the altitude for each shapefile was updated to “clamp it to ground”. This procedure takes the edited shapefile and pairs it to the altitude values of the terrain it overlays. This ensures that measurements using the shapefile correspond with the terrain data and provide accurate volume and profile measurements.

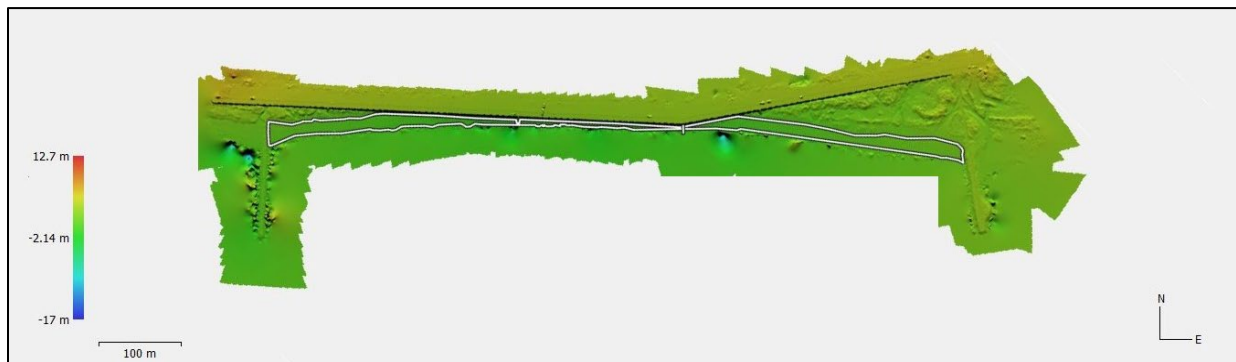


Figure 9 December 2016 digital elevation model (DEM) of Section 1 Beach segment 1 with volume polygon and profile polyline. *Produced using Agisoft Photoscan Pro

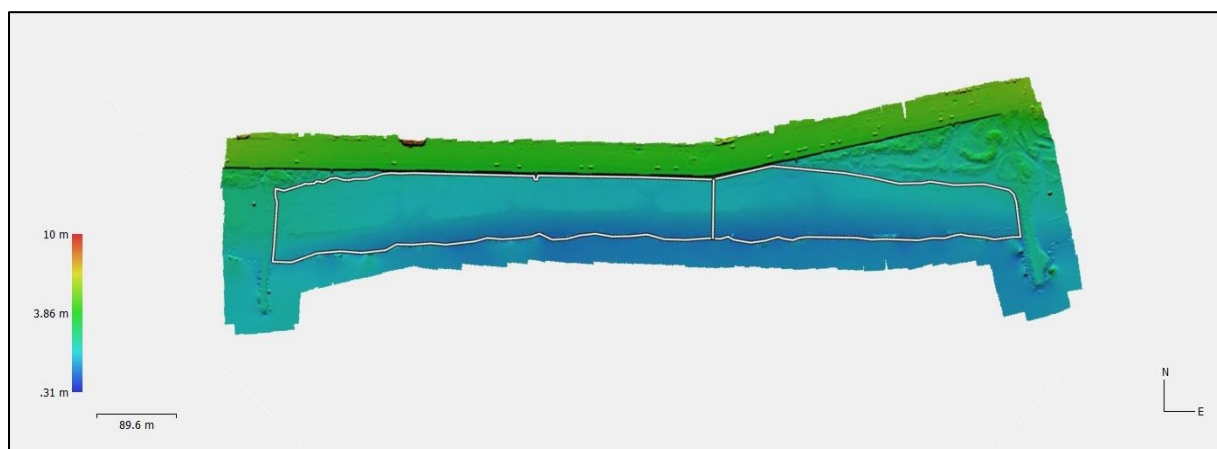


Figure 10 May 2017 DEM of Section 1, Beach segment 1 with volume polygon and profile polyline. *Produced using Agisoft Photoscan Pro

Volume measurements and profiles were then taken for the 12 beach segments for each of the 14 months. The volumes were measured from a baseline which was Mean Sea Level (MSL) 0.3 m for Galveston as measured by NOAA at the Galveston Bay Entrance station 8771341 (Figure 11). Profile measurements were taken the same way as volume measurements using the Profile tool (Figure 12).

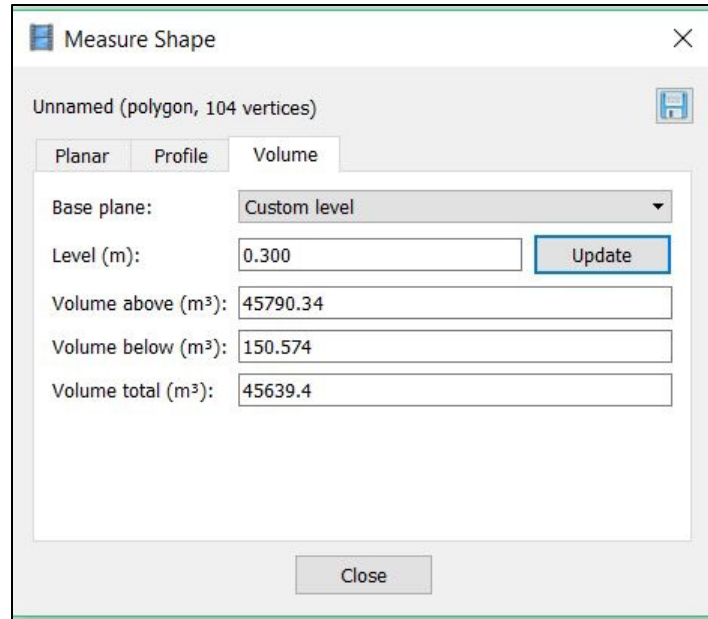


Figure 11 Volume calculation for Section 3, Beach segment 3 using mean sea level (MSL) as the baseline. *Produced using Agisoft Photoscan Pro



Figure 12 Profile measurement for Section 3, Beach segment 3. *Produced using Agisoft Photoscan Pro

Volume and profile data were recorded for each month in Excel and plotted for comparison. An average volume and average profile for the entire 6.2 km study area was

compiled so that the changes in volume and profile could be compared to SWH data to quantify the relationship between monthly SWH and sand volume loss (Figures 13 & 14).

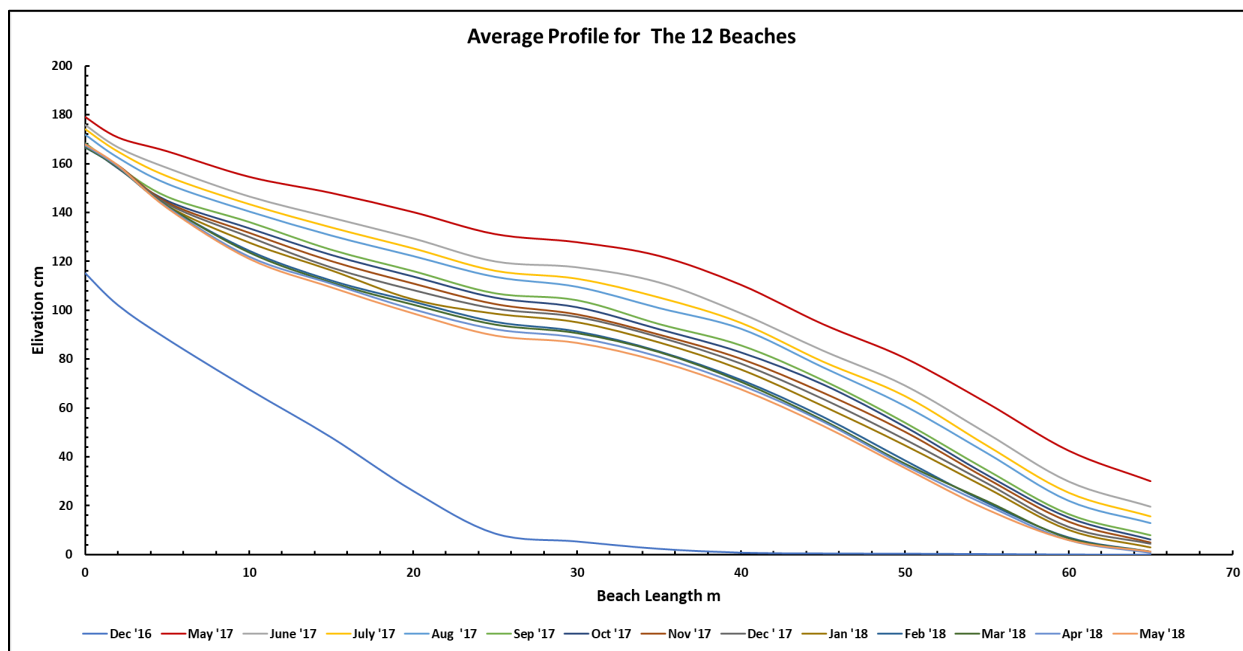


Figure 13 Average beach profile change for the 14 months of the study.

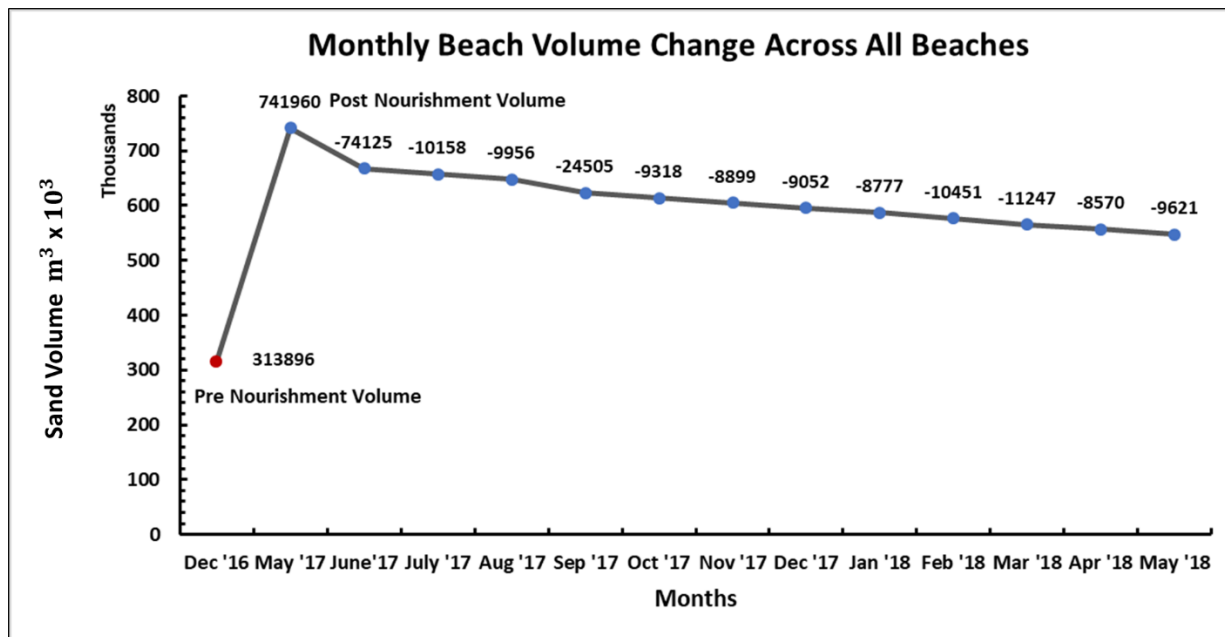


Figure 14 Change in each beach volume and average beach volume for the 14 months of the study. Note The 2.2 km length of beach segments 13* & 14* are estimated volumes as they could not be measured due to overhanging structures.

3.5 Wave Height Data Processing and Analysis

Significant Wave Height (SWH) data for the months of May 2017 through April 2018 was collected from the NOAA National Data Buoy Center (NDBC) for NOAA oceanographic and meteorological buoy LLNR 1200 located 35 km offshore of Galveston and located in 15 m of water. SWH data for May 2018 was unavailable from this buoy at the time of the thesis defense. The SWH is defined by NOAA as the average of the highest one-third of all the wave heights measured during each 20-minute sampling period for each hour. There are on average 730 twenty-minute measurements per month.

The raw SWH for May 2017 through April 2018 was turned into tables in Excel to create histograms of significant wave height/hour over the period of the month. This was done by creating 0.1 m wide bins ranging from 0.0m to 3.6 m (the highest hourly wave for the period examined).

This data was then normalized using the “Standardize” function in Excel so that each monthly data set contained 730 data points. This was done so that each month’s distribution of significant wave height per hour could be compared to the other monthly SWHs and the volume and profile data from the UAS surveys to quantify the relationship between SWH and the change in the beach volume over the 12 months of the study to see if significant erosional events found in the beach fill volume data correlated with a greater number of large waves (Figures 15 & 16).

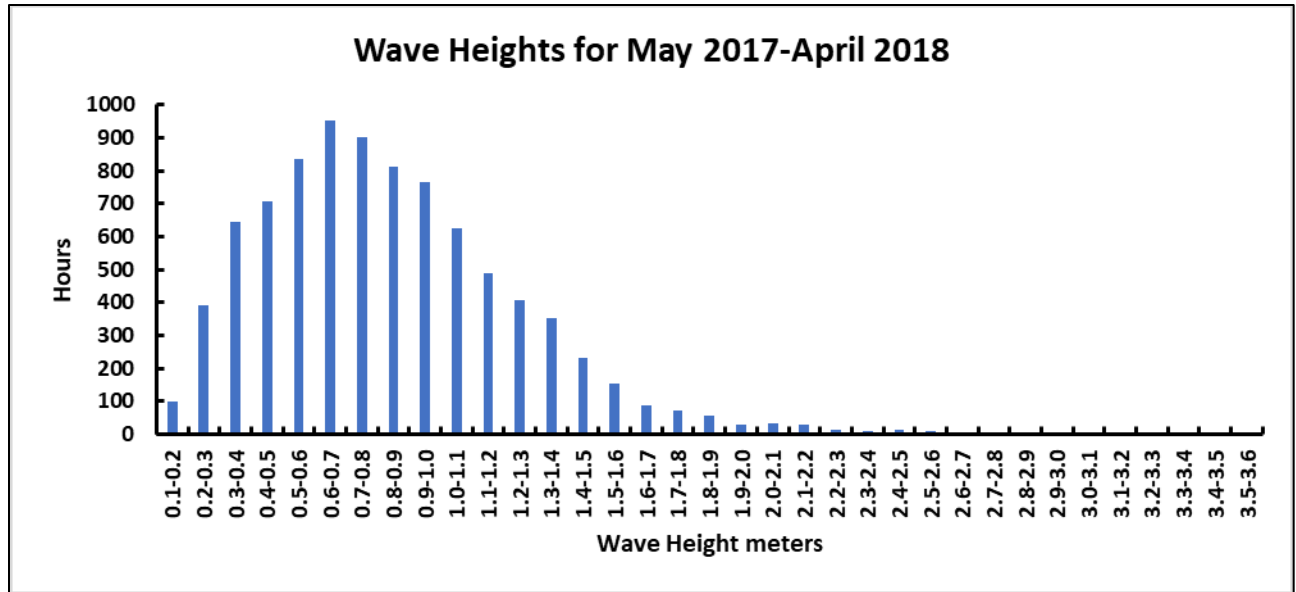


Figure 15 Histogram of SWH per hour for May 2017 through April 2018. Range 0.1-0.2 m to 3.5-3.6 m. Skewness 1.018.

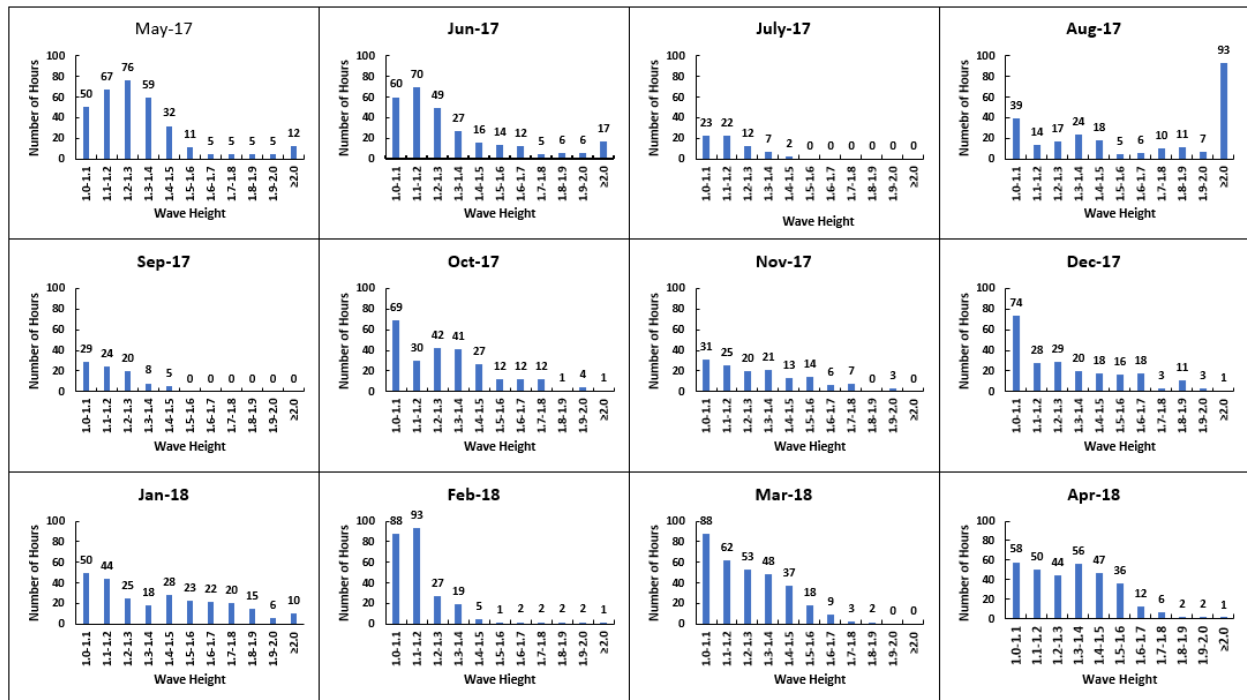


Figure 16 Significant Wave Height and the number of hours they were prevalent. Note the large number of hours (93) with waves over 2.0 m during August 2017 (month of Harvey making landfall) vs the previous month of July 2017 in which no waves were over 1.4 m. The number of hours for waves less than 1.0 m are not shown. Despite making landfall 253 km Southwest of Galveston the storm still influenced SWH at the study area.

The descriptive statistics were then created using the Excel Data Analysis tool box for each month's SWH data to determine the skewness coefficient for each month. A positive skewness shows that rather than a normal Rayleigh distribution typical of wave height statistics found in spectral wave analysis, there were a greater number of waves whose height was anomalous for that month. The skewness values ranged from -0.02 (March 2018) to 1.50 (August 2017).

Additionally, the monthly percent loss was calculated for the average beach volume of the study area. The percent volume losses for May 2017 (0%) and June 2017 (9.9%) were removed for this comparison as May 2017 being the last month of the active nourishment project has no loss and the loss seen for June 2017 was exacerbated by the expected settling and loss of the component of the beach nourishment called the "equilibration fill" (Figure 17) as it is moved offshore from the beach to below the Mean Low Low Water Line (MLLW) (Willson, Thomson, Roberts Briggs, Elko, & Miller, 2017).

The SWH skewness numbers were then advanced 1 month forward to reflect the difference in how volume measurements and wave data were recorded. Monthly volume measurements represent the difference in change between 2 months, except for May 2017 when the fill was completed and SWH data represents the actual conditions during the month. It was essential to match the two data sets with a time step in order to compare conditions during the month to its recorded volume change (Table1).

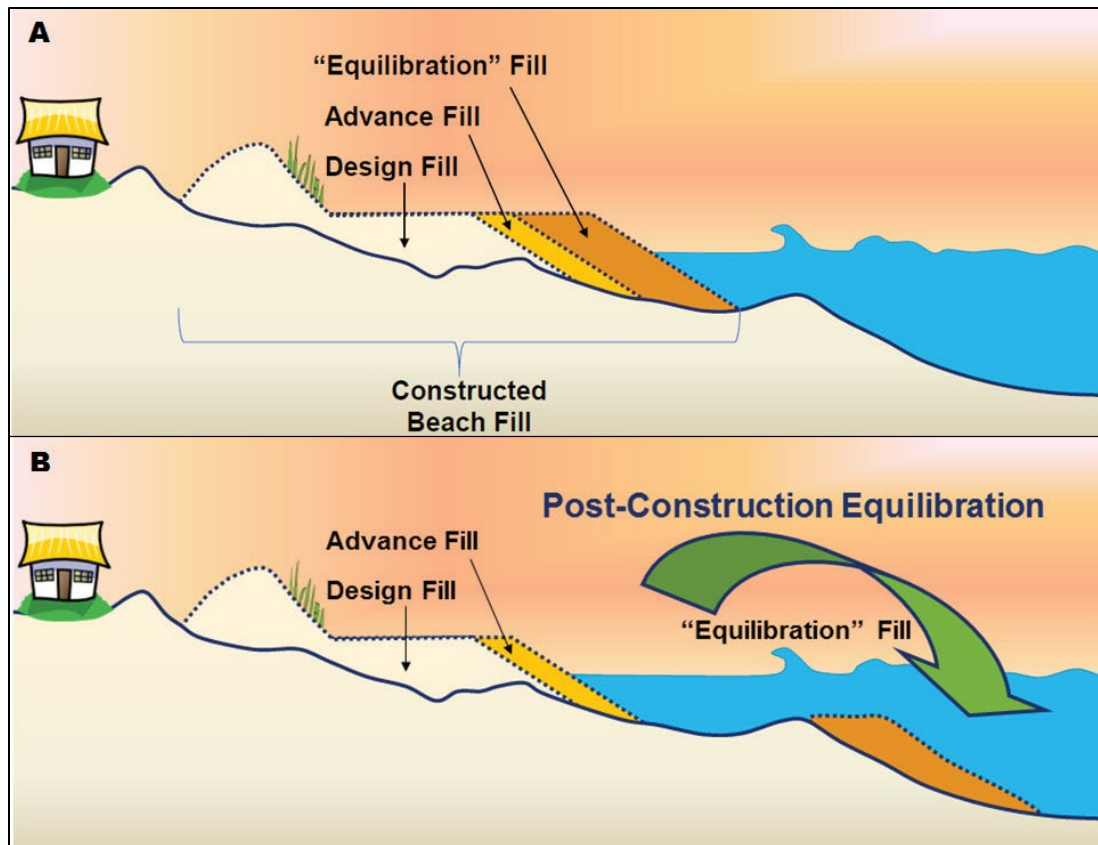


Figure 17 Components of beach nourishment projects designed to erode at different rates. Reprinted from “Beach nourishment profile equilibration: What to expect after sand is placed on a beach.” K. Willson, 2017. *Shore & Beach*, 85 No. 2, 50. Copyright [2017] by *Shore & Beach*.

Table 1. Monthly Average Volume Data and Significant Wave Height Skewness Coefficients. Note: Monthly volume measurements represent the difference in change between 2 months, except for May 2017, SWH is for the month recorded.

Month	Averaged Beach Volume Cubic meters	% Average Loss	Monthly SWH Skew
May '17	741960	0.00	0
June '17	667835	9.90%	0.27
July '17	657677	1.46%	0.68
Aug '17	647720	1.41%	0.85
Sep '17	623215	3.62%	1.50
Oct '17	613896	1.42%	0.74
Nov '17	604997	1.34%	0.44
Dec '17	595944	1.25%	0.99
Jan '18	587167	1.32%	0.67
Feb '18	576716	1.71%	0.66
Mar '18	565468	1.69%	-0.02
Apr '18	556898	1.98%	0.10
May '18	547276	1.50%	0.02

3.6 Ground Truthing

In order to assess the accuracy of measurements being made using the UAS, a test was devised in which a single beach segment would be imaged with the UAS using optimal flight and measurement parameters (see **Appendix A**) and compared with an RTK GPS profile measured right after the UAS flight. A survey tape was laid out on the beach from the base of the Seawall to the waterline to use so that RTK and UAS-based measurements could be made along the same profile and at an equal 1 m spacing along the tape. Sixty RTK measurements were recorded along the profile, points were then drawn in the UAS data for the survey along the base line to match the 1 m portions taken with the RTK, measurements of the position and elevation were then made for each point in the UAS data using the Measure Shape tool in Agisoft Photoscan Pro. This test showed that there was a maximum difference of +/- 2 cm between UAS and RTK measurements made along the profile with <1 cm being the most common (Figure 18 & **Appendix C**).

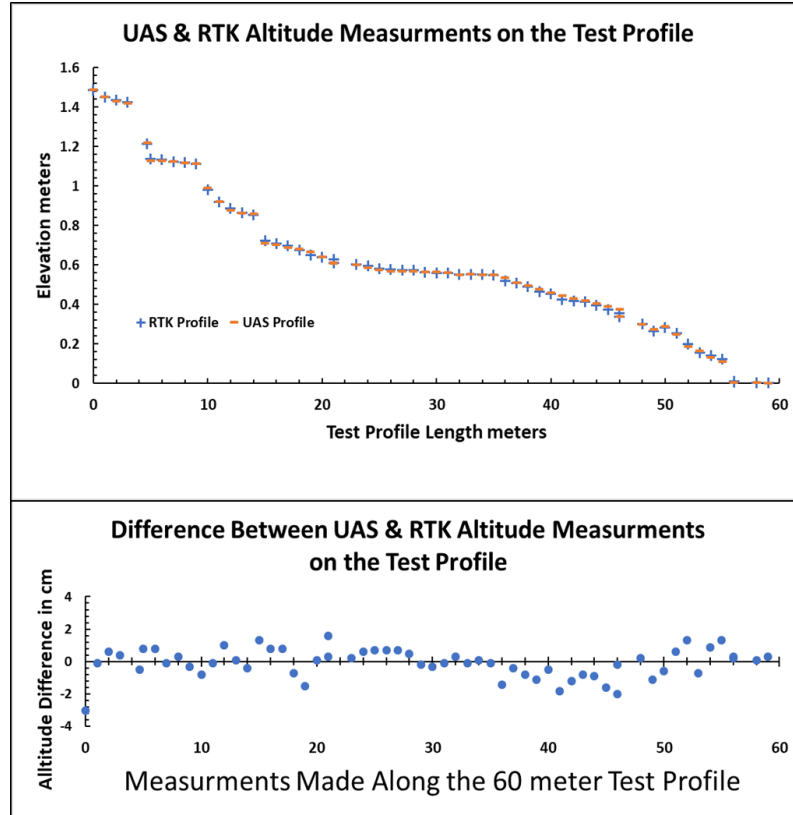


Figure 18 Difference in altitude measurements taken by RTK and UAS along the profile line used for ground truth testing. Note: Measurements were made at 1 meter intervals along a single profile extending from the base of the Seawall (0 m) to the water line (60 m).

4. RESULTS

4.1 Introduction

The use of UAS-based photogrammetry to survey the Phase III Beach Nourishment: Seawall East project from May 2017 to May 2018, produced high-resolution data of the subaerial beach that documented volume and profile change efficiently. The use of the developed deployment protocol (Appendix A) in conjunction with the ability to use GCPs in the hard structures of the study area created a system in which the imaging phase of the project took only a few hours per day over three days per month to survey the entire 133-hectare area.

4.2 Volume Change and Nourishment Lifespan

Volume change and profile change measurements of the 12 subaerial beach segments studied pre- (December 2016) and post- (May 2017- May 2018) nourishment documented the rate of loss to the fill and the change to the profile of these beaches.

Beach nourishment projects are designed with several fill components, each designed to erode at a different rate (Figure 17). The total volume of sand placed on the beach is referred to as the “constructed fill”. The components making up the constructed fill are the “design fill” which is the portion of the volume of sand used to achieve the planning goal (i.e. to achieve a certain beach width). The “advanced fill” which is added to the design fill as a volume of sand measured to match the long-term erosion rate of the shoreline to meet the designs project lifespan. Finally, there is an “equilibration fill”, which is part of the construction process and allows the design and advanced fill to be placed. After the project is complete the equilibration fill erodes quickly due to its steep slope and is redistributed to the subaqueous portion of the beach profile (Dean, R. G., 1987; Dean, Robert G., 1991; Willson et al., 2017). It is important to note that sand moved along the profile from the subaerial area to subaqueous area or alongshore

is not 'lost' (Dean, Cory, 1989; Dean, R. G., 1987) This process was seen in the volume change from May 2017-June 2017 when the average monthly rate of volume loss was 9.9%.

Averaging this data into a single volume and profile change for the entire 6.2 km allowed for the calculation of the month-by-month percentage of fill lost post-nourishment. This rate of loss curve can be extrapolated to estimate the expected time (in months) before the beach would return to its pre-nourishment volume (Figures 19 & 20).

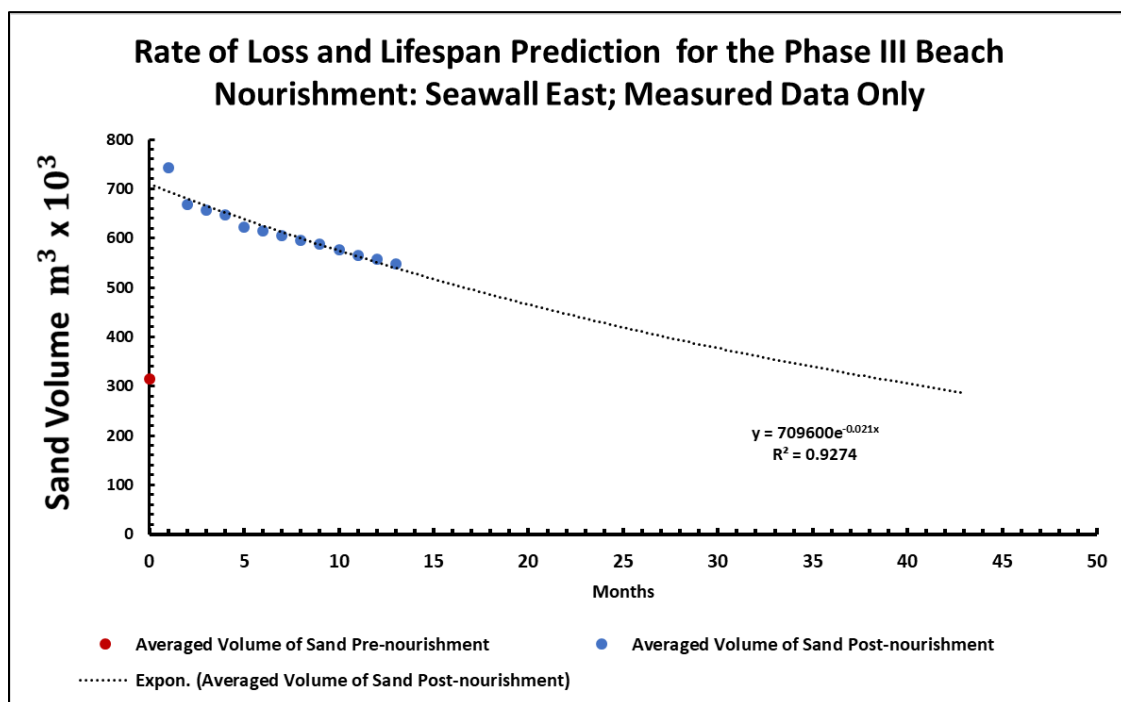


Figure 19 Rate of loss and lifespan prediction for the Phase III Beach Nourishment Project.
Note: Percentage of fill lost thru May 2018 was 26.2%

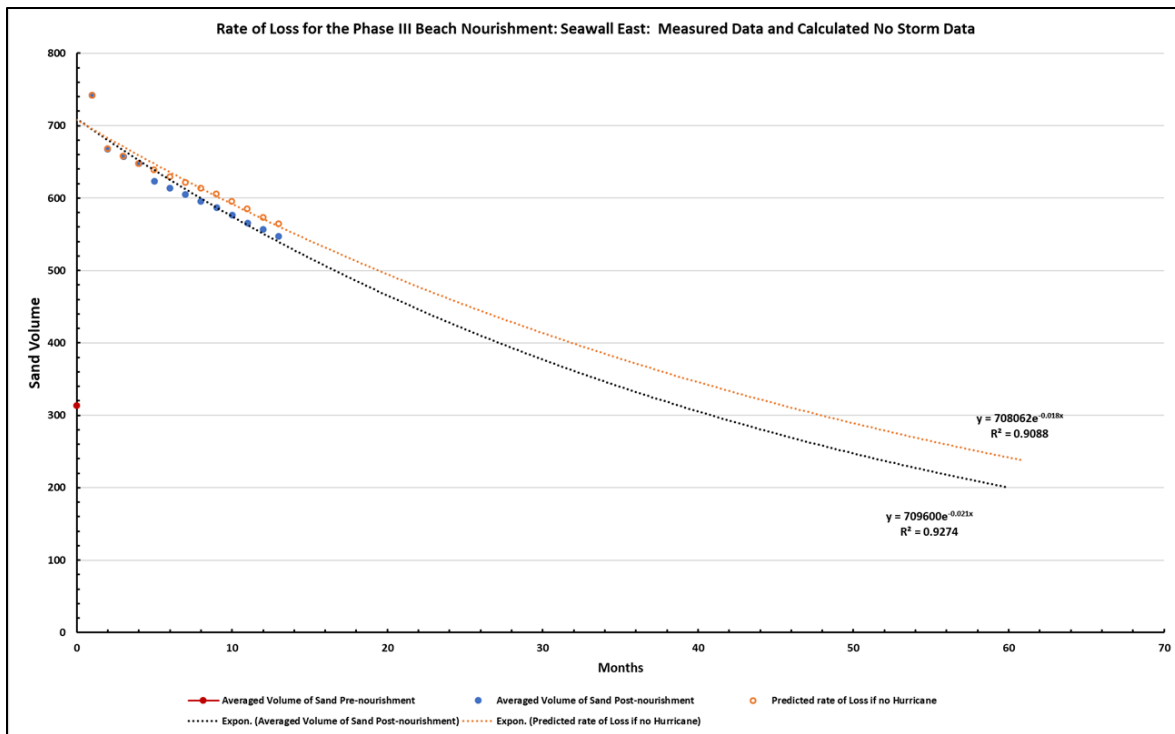


Figure 20 Rate of loss and lifespan prediction (with & without hurricane) for the Phase III Beach Nourishment Project. Note: Percentage of fill lost thru May 2018 was 26.2%. Percentage of fill lost if back-stripping tropical storm effects was 15.7%

Additionally, the rate of loss and lifespan prediction was calculated for the nourishment if Hurricane Harvey had not occurred during the study period. These calculations of lifespan show that at the current rate of loss (26.2% per year) the subaerial beach will return to its pre-nourishment volume in ~42 months (3.5 years). If the beach had not been impacted by extreme weather events the calculated rate of loss (15.7% per year) means that the subaerial beach should have had a life span of ~54 months (4.5 years). This 4.5 year no storm lifespan calculation for the study area in Reach 1 is roughly consistent with a 5-year nourishment cycle recommended by USACE based on simulations the GenCade numerical model. USACE in their Galveston Island, Texas, Sand Management Strategies to develop the Phase III Beach Nourishment: Seawall East

plan recommended a 0.76 million m³ to 1.53 million m³ nourishment every 5 years to maintain the shoreline (Frey et al., 2016)(Table 2).

Table 2. List of USACE GenCade model output alternatives for Galveston Island restoration for Reach 1 (yellow), Adapted from “Galveston Island, Texas, Sand Management Strategies.” by A. E. Frey, 2016, (Technical Report No. ERDC/CHLTR-16-13), 88. Coastal and Hydraulics Laboratory: U.S. Army Engineer Research and Development Center. Note: Measurements made by USACE are in Imperial units.

	Source Term = 0K yd ³ /year	Source Term = 180K yd ³ /year	Source Term = 356K yd ³ /year	Reach 1	Reach 1 and Reach 2
No Action	X	X	X		
Structural Alternatives					
Groin Modifications		X			
Sand Tighten Jetty		X	X		
Beach Fills - Seawall Grid					
125K yd ³ /year		X		X	
100K yd ³ /5 year		X		X	
250K yd ³ /2 year	X	X	X	X	X
500K yd ³ /2 year		X		X	X
1 M yd ³ /2 year		X		X	X
500K yd ³ /5 year		X		X	X
1 M yd ³ /5 year		X		X	X
2 M yd ³ /5 year		X		X	X
Large-Scale Beach Fill				X	X

4.3 Volume Change and Relationship to Significant Wave Height

The month of highest volume loss (August 2017) was correlated with the month of greatest number of hours (93) of SWH >2.0 m. This was significantly above average for wave conditions found for the other 11 post-nourishment months (Figure 21).

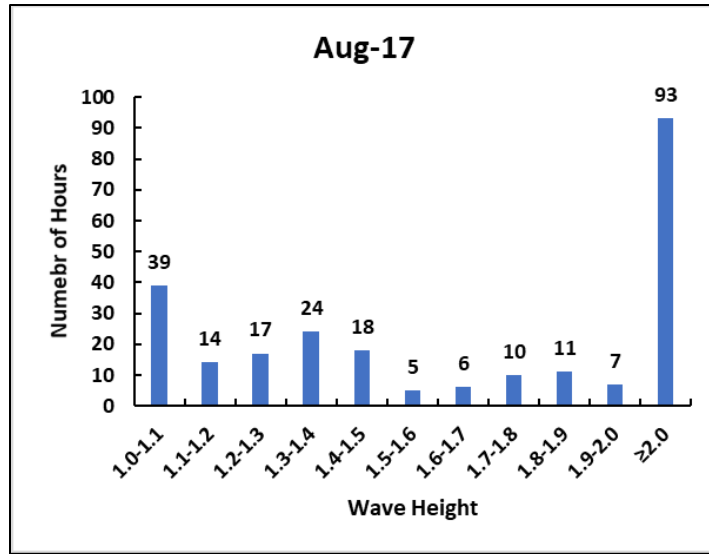


Figure 21 Hourly significant wave height for the month of August 2017 when Hurricane Harvey occurred. Compare with the other months shown in figures 15 & 16.

The average monthly percentage loss rate when compared to SWH skewness showed that SWH, (especially the SWH influenced by Hurricane Harvey) was a forcing agent for erosion of the subaerial beach (Figure 22). While a more detailed study of Reach 1 is required to determine a set of parameters for all forcing agents affecting erosion in the groin field (e.g. longshore transport, wind direction and speed, wave direction, and rainfall) this preliminary observation provides evidence that storm surge, low atmospheric pressure, and high winds contributing to extreme SWH for long periods will shorten the life span of beach nourishment projects on Galveston by a factor of years (Figure 20). All other months showed that the percentage loss rate is constant at $1.4 \pm 0.5\%$ irrespective of SWH skewness values less than 1.0, only values greater than 1.0 start to exhibit enhanced loss rates (Figure 22).

The SWH for September 2008 when Hurricane Ike made landfall on Galveston Island was analyzed using the same methods as the 2017-2018 SWH data. The Hurricane Ike event generated 34 hours of waves over 3 m with 13 of those hours generating waves over 5 m. By

comparison, Hurricane Harvey generated 13 hours of waves over 3 m which was the maximum SWH for the storm event. When Hurricane Ike struck Galveston the last time the Seawall area had been nourished was in 1995 when 0.76 million m³ was placed in the groin field and by 1997 this fill had nearly reached its pre-equilibrium profile (Ravens & Sitanggang, 2007b). At the time of Ike's land fall it is not known exactly how much of this fill was left after 13 years but conservative estimates suggest that roughly 91% of the fill from 1995 had been eroded by September 2008. After Hurricane Ike, it was estimated that 90-100% of the remaining fill had been lost which was used to justify an emergency nourishment project in 2009. Taking the conservative estimate of 90% it was calculated that Ike would have eroded at least 10% of a full nourishment project fill like the one completed in 2017.

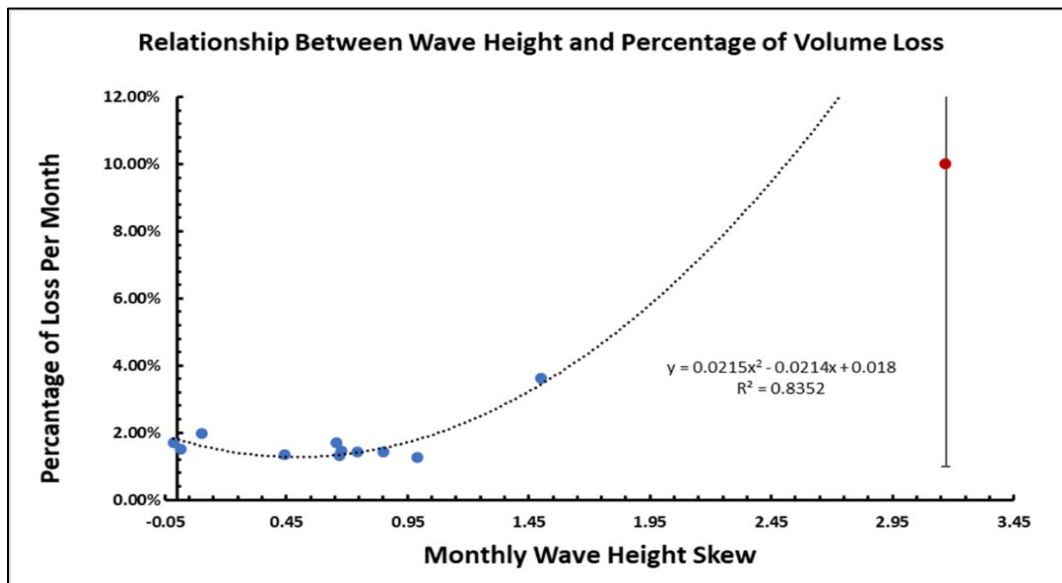


Figure 22 Relationship between monthly SWH skewness and monthly fill volume loss rate. Note the insensitivity of loss rate for SWH skewness values less than 1.0. This constancy allows greater confidence in extrapolating cumulative loss rates to predict timing of the next nourishment projects. The red data point represents Hurricane Ike, September 2008, where it was estimated it caused 10% erosion with a 3.17 monthly SWH skewness for September.

4.4 Feature Recognition

DEMs and orthomosaics allowed for the identification of features in the beach and their creation or change over the study period. Seawall Boulevard sheds rain over Galveston's Seawall and several associated features of the Seawall such as stairs, ramps, and drains funnel this water onto the beach. This action creates erosional cuts in the beach, carrying away beach material and exacerbating subaerial erosion (Figure 23). Events of heavy rain followed by dry periods where wind and pedestrian traffic on the beach had a chance to fill these erosional cuts can be seen. While some of these cuts are quite wide and deep and will remain for some time, smaller cuts were easily filled and little evidence of them remains today. By recording and measuring this type of feature with UAS allows for more accurate and precise beach volumes than with standard RTK GPS surveys which do not have the areal coverage to resolve these features.

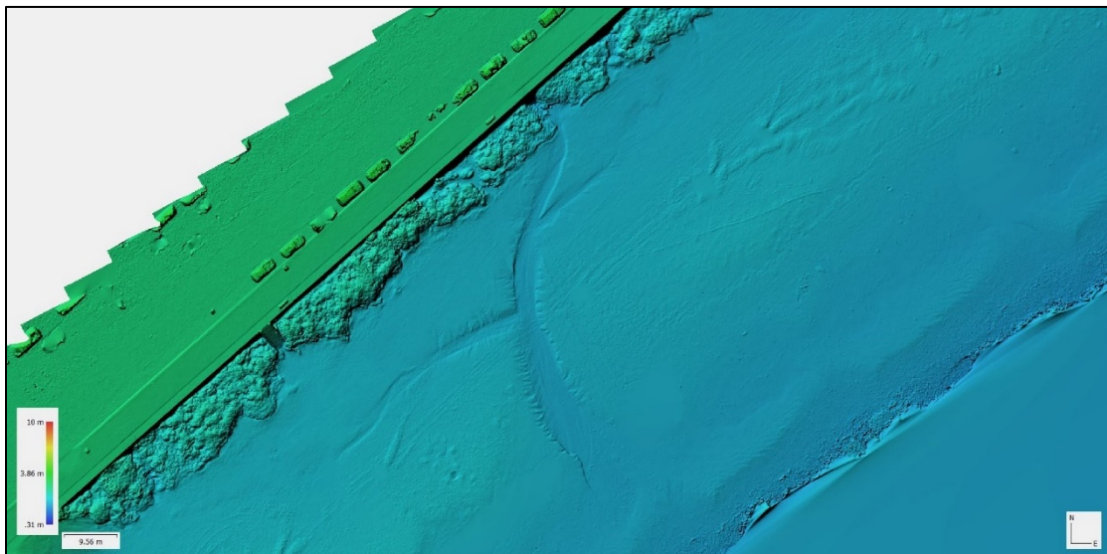


Figure 23 Example of an erosional cut in Section 2, Beach segment 2 July 2017. *Produced using Agisoft Photoscan Pro

5. DISCUSSION

This study of the change of volume and profile of the subaerial area of newly nourished beaches, using UAS-based photogrammetry shows that monthly measurements of these beaches in their first year can determine their lifespan. This has broad implications for local, state, and federal coastal managing agencies tasked with planning, funding, and maintaining their beaches. The development of a standardized deployment protocol using a consumer-grade UAS to derive highly accurate elevational measurements for use in beach surveys along with the ease of use of UAS technology makes multi-month studies like this one convenient and practical.

This study was able to document monthly volume change and quantify the impact of events such as Hurricane Harvey. The fill volume lost from May 2017-May 2018 was 26.2%. This compared with an estimated 15.7% fill loss in the first year if the effects of Hurricane Harvey were removed. Extrapolating these trends leads to a projected lifespan of the subaerial beach to be 3.5 and 4.5 years respectively. The implication of this is that the next nourishment cycle for the Reach 1 beach area will need to be funded, planned, and fill material sourced sooner than estimated by the Corps of Engineers GenCade model. It is important to note that the subaerial beach is the dry portion of the beach that contains the dunes and berm, and that much of what is technically considered a beach also extends subaqueously to the depth of closure. Measurements on beach material below the waterline during low tide was not collected and therefore this data cannot speak for the whole beach. The data on the subaerial beach alone is just as valuable and is more easily related to coastal zone managers and the public since this is the most visible portion of the beach and erosion is more evident (Cook, 2017; Gonçalves & Henriques, 2015; Nikolakopoulos et al., 2017; Turner, Harley, & Drummond, 2016).

UAS-based photogrammetry presents a less expensive, yet highly efficient, alternative to traditional survey methods for monitoring beach nourishments such as the Phase III Beach Nourishment: Seawall East. The methodology described in this thesis and its application has the potential to allow coastal managers and planners to make accurate measurements in a time frame that will allow them to plan accordingly to change conditions at their shorelines. The ability to rapidly incorporate data on the effect of extreme or anomalous weather events can give these managers data for erosion mitigation planning in near real time.

An excellent example of the utility of using the UAS protocol developed here was the ability to rapidly respond to tropical storms and hurricanes as they interacted with the Gulf Coast during the summer of 2017. After Hurricane Harvey dissipated and airspace regulations allowed, flights to survey the impact the storm had on the beach were conducted on September 2nd-5th. This data was invaluable in measuring the change to the volume of the nourished beach and the calculation of its longevity.

The methodology used for this thesis and the data collected has been shown-to provide information that can be applied to many coastal problems and allow for the study of other forcing factors that impact sandy beaches. Considering that sea-level rise and coastal erosion are issues affecting coastal communities, shore line recession is an issue that will have to be taken into account for future nourishment projects worldwide. Roughly 31% of the world's ice-free beaches are sandy, and of this number 24% are eroding at a rate of 0.5 m a year (Luijendijk et al., 2018). While not all of these are tourist beaches, like those of Galveston Island, this erosional rate is more visible to the public in areas with higher populations and where the local economy based on beach tourism warrants nourishment projects. At a cost of \$19.1 million the Phase III Beach Nourishment: Seawall East project was one of Texas's most costly and ambitious nourishment

projects to-date. Incorporating UAS-based photogrammetry into traditional studies of the effects of longshore transport, wind, tidal fluctuations, and sea level rise on beach erosion is a desired avenue of future research. This is important for understanding the process of equilibration that nourished beaches undergo and could help refine beach nourishment and erosional planning/forecasting.

Continued study of the Phase III Beach Nourishment: Seawall East using the methods outlined in this thesis is required to develop a full understanding of the long-term impacts of forcing agents and extreme weather events to beach longevity. Using a system of first year monthly surveys, like those described here, then moving to quarterly surveys until either the beach returns to its pre-nourishment state or the event of the next nourishment fill should provide a detailed description of how the subaerial beaches equilibrate under Galveston's unique coastal influences in the presence of a groin field.

6. CONCLUSION

This thesis employed empirical methods to develop a standardized deployment protocol for deriving accurate elevational measurements for UAS-based beach surveys that surpasses RTK GPS based methodologies for surveying beaches in its level of detail and ease of use. This methodology was able to quantify both the change in volume and profile of a beach and to provide a better understanding of the “normal” on-going erosion rate and the impact of an extreme weather event on the newly nourished beach and their combined effect on the estimated lifespan of the Phase III Beach Nourishment: Seawall East project. This nourishment project was designed to maintain the shoreline in this section of the Galveston Seawall for approximately 4.5-5 years but due to the impacts of Hurricane Harvey this study found that it was deduced to 3.5 years. This thesis shows that using UAS-based photogrammetry in conjunction with the developed protocol has the potential to provide coastal managing agencies with timely, high-resolution data needed to make informed decisions concerning the state of their beaches for a lower cost and effort than traditional beach survey methods.

In order to better manage nourishment cycles, high-resolution data derived from new technology and methods like UAS based photogrammetry and the deployment protocol described in this thesis, should be used to monitor both nourished and non-nourished beaches in areas where economic and environmental concerns guide coastal management practices. Beach nourishment projects are usually required to be monitored on at least an annual basis as part of the permitting processes with state and Federal agencies. Often these monitoring surveys are conducted by the company or organization that was hired to design and conduct the nourishment. This situation often leads to monitoring conducted only at the minimum required intervals or

directly after a severe weather event. These long gaps in reliable data on the health of managed beaches puts coastal managers at a disadvantage when it comes to planning future nourishments.

UAS and the protocol developed for their deployment for this thesis research are powerful tools that can be put in the hands of coastal managers to facilitate informed decision making in monitoring ongoing, and planning future, beach nourishment projects. Projects that require significant amounts of both funding and sand resources.

REFERENCES

- Baltsavias, E. P. (1999). A comparison between photogrammetry and laser scanning. *ISPRS Journal of Photogrammetry and Remote Sensing*, 54(2-3), 83-94. doi:10.1016/s0924-2716(99)00014-3
- Boon, M. A., Greenfield, R., & Tesfamichael, S. (2016). Wetland assessment using unmanned aerial vehicle (uav) photogrammetry. *ISPRS - International Archives of the Photogrammetry, Remote Sensing and Spatial Information Sciences*, XLI-B1, 781-788. doi:10.5194/isprs-archives-xli-b1-781-2016
- Boon, M. A., Greenfield, R., & Tesfamichael, S. (2016). Unmanned aerial vehicle (UAV) photogrammetry produces accurate high-resolution orthophotos, point clouds and surface models for mapping wetlands. *South African Journal of Geomatics*, 5(2), 186-200. doi:10.4314/sajg.v5i2.7
- Casella, E., Rovere, A., Pedroncini, A., Mucerino, L., Casella, M., Cusati, L. A., . . . Firpo, M. (2014). Study of wave runup using numerical models and low-altitude aerial photogrammetry: A tool for coastal management. *Estuarine, Coastal and Shelf Science*, 149, 160-167. doi:10.1016/j.ecss.2014.08.012
- Colomina, I., & Molina, P. (2014). Unmanned aerial systems for photogrammetry and remote sensing: A review. *ISPRS Journal of Photogrammetry and Remote Sensing*, 92, 79-97. doi:10.1016/j.isprsjprs.2014.02.013
- Cook, K. L. (2017). An evaluation of the effectiveness of low-cost UAVs and structure from motion for geomorphic change detection. *Geomorphology*, 278, 195-208. doi:10.1016/j.geomorph.2016.11.009
- Daponte, P., Vito, L. D., Mazzilli, G., Picariello, F., & Rapuano, S. (2017). A height measurement uncertainty model for archaeological surveys by aerial photogrammetry. *Measurement*, 98, 192-198. doi:10.1016/j.measurement.2016.11.033
- Dean, C. (1989,). **As beach erosion accelerates, remedies are costly and few.** *The New York Times* Retrieved from <https://www.nytimes.com/1989/08/01/science/as-beach-erosion-accelerates-remedies-are-costly-and-few.html>
- Dean, R. G. (1986). *Coastal armoring: Effects, principles and mitigation*
doi:doi:10.1061/9780872626003.135
- Dean, R. G. (1987). **Additional sediment input to the nearshore region.** *Shore & Beach*, 55, 76-81.
- Dean, R. G. (1991). Equilibrium beach profiles: Characteristics and applications. *Journal of Coastal Research*, 7(1), 53-84. Retrieved from <http://www.jstor.org/stable/4297805>

- Frey, A. E., Morang, A., & King, D. B. (2016). *Galveston Island, Texas, Sand Management Strategies*. (Technical Report No. ERDC/CHLTR-16-13). Coastal and Hydraulics Laboratory U.S. Army Engineer Research and Development Center 3909 Halls Ferry Rd Vicksburg, MS 39180-6199: The U.S. Army Engineer Research and Development Center (ERDC). Retrieved from <https://erdc-library.erdcdren.mil/xmlui/handle/11681/20297>
- Gonçalves, J. A., & Henriques, R. (2015). UAV photogrammetry for topographic monitoring of coastal areas. *ISPRS Journal of Photogrammetry and Remote Sensing*, 104, 101-111. doi:10.1016/j.isprsjprs.2015.02.009
- Google Earth. (2018). *V. 7.1.8.3036 2017. Galveston Island Texas 29°16'41.85"N, 94°48'15.25"W, elevation 7km. viewed 31 August 2018.* <http://Www.google.com/earth/index.html>>
- Hugenholtz, C. H., Whitehead, K., Brown, O. W., Barchyn, T. E., Moorman, B. J., LeClair, A., . . . Hamilton, T. (2013). Geomorphological mapping with a small unmanned aircraft system (sUAS): Feature detection and accuracy assessment of a photogrammetrically-derived digital terrain model. *Geomorphology*, 194, 16-24. doi:10.1016/j.geomorph.2013.03.023
- Jones, A. R., Schlacher, T. A., Schoeman, D. S., Weston, M. A., & Withycombe, G. M. (2017). Ecological research questions to inform policy and the management of sandy beaches. *Ocean & Coastal Management*, 148, 158-163. doi:10.1016/j.ocecoaman.2017.07.020
- King, D. B. (2007). *Wave and beach processes modeling for sabine pass to galveston bay, texas, shoreline erosion feasibility study*. (Final Report No. ADA471889). DEFENSE TECHNICAL INFORMATION CENTER: ENGINEER RESEARCH AND DEVELOPMENT CENTER VICKSBURG MS COASTAL AND HYDRAULICS LAB. Retrieved from <http://www.dtic.mil/docs/citations/ADA471889>
- Long, N., Millecamps, B., Pouget, F., Dumon, A., Lachaussée, N., & Bertin, X. (2016). Accuracy assessment of coastal topography derived from uav images. *ISPRS - International Archives of the Photogrammetry, Remote Sensing and Spatial Information Sciences, XLI-B1*, 1127-1134. doi:10.5194/isprs-archives-xli-b1-1127-2016
- Luijendijk, A., Hagenaars, G., Ranasinghe, R., Baart, F., Donchyts, G., & Aarninkhof, S. (2018). The state of the worlds beaches. *Scientific Reports*, 8(1), 6641. doi:10.1038/s41598-018-24630-6
- Matese, A., Toscano, P., Gennaro, S. F. D., Genesio, L., Vaccari, F. P., Primicerio, J., . . . Gioli, B. (2015). Intercomparison of UAV, aircraft and satellite remote sensing platforms for precision viticulture. *Remote Sensing*, 7(3), 2971-2990. doi:10.3390/rs70302971
- Nex, F. & Remondino, F. (2014). **UAV for 3D mapping applications: A review**. *Applied Geomatics*, 6(1), 1-15. doi:<https://doi.org/10.1007/s12518-013-0120-x>

- Nikolakopoulos, K. G., Kozarski, D., & Kogkas, S. (2017). Coastal areas mapping using UAV photogrammetry. *10428*, 1042800. doi:10.1117/12.2278121
- Nikolakopoulos, K. G., Soura, K., Koukouvelas, I. K., & Argyropoulos, N. G. (2017). UAV vs classical aerial photogrammetry for archaeological studies. *Journal of Archaeological Science: Reports*, *14*, 758-773. doi:10.1016/j.jasrep.2016.09.004
- Papakonstantinou, A., Topouzelis, K., & Pavlogeorgatos, G. (2016). Coastline zones identification and 3D coastal mapping using UAV spatial data. *ISPRS International Journal of Geo-Information*, *5*(6), 75. doi:10.3390/ijgi5060075
- Qin, R., Tian, J., & Reinartz, P. (2016). 3D change detection “approaches and applications. *ISPRS Journal of Photogrammetry and Remote Sensing*, *122*, 41-56. doi:10.1016/j.isprsjprs.2016.09.013
- Ravens, T. M., & Sitanggang, K. I. (2007a). Numerical modeling and analysis of shoreline change on galveston island. *Journal of Coastal Research*, *23*(3), 699-710. Retrieved from <http://www.jstor.org/stable/4494239>
- Ravens, T. M., & Sitanggang, K. I. (2007b). Numerical modeling and analysis of shoreline change on galveston island. *Journal of Coastal Research*, *23*(3), 699-710. doi:10.2112/04-0191.1
- Rusnák, M., Sládek, J., Kidová, A., & Lehotský, M. (2018). Template for high-resolution river landscape mapping using UAV technology. *Measurement*, *115*, 139-151. doi:10.1016/j.measurement.2017.10.023
- Scarelli, F. M., Sistilli, F., Fabbri, S., Cantelli, L., Barboza, E. G., & Gabbianelli, G. (2017). Seasonal dune and beach monitoring using photogrammetry from UAV surveys to apply in the ICZM on the ravenna coast (emilia-romagna, italy). *Remote Sensing Applications: Society and Environment*, *7*, 27-39. doi:10.1016/j.rsase.2017.06.003
- Siebert, S., & Teizer, J. (2014). Mobile 3D mapping for surveying earthwork projects using an unmanned aerial vehicle (UAV) system. *Automation in Construction*, *41*, 1-14. doi:10.1016/j.autcon.2014.01.004
- Songy, G. (2017). Completion of texas' largest-ever beach Nourishment Along Galveston seawall. Paper presented at the Retrieved from http://www.texasasbpa.org/site/wp-content/uploads/2017/05/TexasASBPA_Symposium_Presentation_Songy.pdf
- Texas General Land Office Coastal Resources Office. (2017). Galveston seawall beach nourishment. Retrieved from <http://www.glo.texas.gov/coastal-grants/projects/1566-galveston-seawall-beach-nourishment.html>
- Todd Davison, A., Nicholls, R. J., & Leatherman, S. P. (1992). Beach nourishment as a coastal management tool: An annotated bibliography on developments associated with the artificial

- nourishment of beaches. *Journal of Coastal Research*, 8(4), 984-1022. Retrieved from <http://www.jstor.org/stable/4298052>
- Tonkin, T. N., Midgley, N. G., Graham, D. J., & Labadz, J. C. (2014). The potential of small unmanned aircraft systems and structure-from-motion for topographic surveys: A test of emerging integrated approaches at cwm idwal, north wales. *Geomorphology*, 226, 35-43. doi:10.1016/j.geomorph.2014.07.021
- Toth, C., & Grzegorz, J. (2016). Remote sensing platforms and sensors: A survey. *ISPRS Journal of Photogrammetry and Remote Sensing*, 115, 22-36. doi:10.1016/j.isprsjprs.2015.10.004
- Turner, I. L., Harley, M. D., & Drummond, C. D. (2016). UAVs for coastal surveying. *Coastal Engineering*, 114, 19-24. doi:10.1016/j.coastaleng.2016.03.011
- Turner, I. L., Harley, M. D., Short, A. D., Simmons, J. A., Bracs, M. A., Phillips, M. S., & Splinter, K. D. (2016). A multi-decade dataset of monthly beach profile surveys and inshore wave forcing at narrabeen, australia. *Scientific Data*, 3, sdata201624. doi:10.1038/sdata.2016.24
- USACE. (1992). *Galveston beach groin field maintenance material placement*. (Section 22). United States Army Engineer District, Galveston Texas: Retrieved from ShoreNet Retrieved from <https://tamug-ir.tdl.org/handle/1969.3/28473>
- Watanabe, Y., & Kawahara, Y. (2016). UAV photogrammetry for monitoring changes in river topography and vegetation. *Procedia Engineering*, 154, 317-325. doi:10.1016/j.proeng.2016.07.482
- Weiss, M., & Baret, F. (2017). Using 3D point clouds derived from UAV RGB imagery to describe vineyard 3D macro-structure. *Remote Sensing*, 9(2), 111. doi:10.3390/rs9020111
- Westoby, M. J., Brasington, J., Glasser, N. F., Hambrey, M. J., & Reynolds, J. M. (2012). Structure-from-motion photogrammetry: A low-cost, effective tool for geoscience applications. *Geomorphology*, 179, 300-314. doi:10.1016/j.geomorph.2012.08.021
- Whitehead, K., & Hugenholtz, C. H. (2014). Remote sensing of the environment with small unmanned aircraft systems (UASs), part 1: A review of progress and challenges. *Journal of Unmanned Vehicle Systems*, 02(03), 69-85. doi:10.1139/juvs-2014-0006
- Willson, K., Thomson, G., Roberts Briggs, T., Elko, N., & Miller, J. (2017). Beach nourishment profile equilibration: What to expect after sand is placed on a beach. *Shore & Beach*, 85 No. 2, 50-51.
- Yahyanejad, S., & Rinner, B. (2015). A fast and mobile system for registration of low-altitude visual and thermal aerial images using multiple small-scale UAVs. *ISPRS Journal of Photogrammetry and Remote Sensing*, 104, 189-202. doi:10.1016/j.isprsjprs.2014.07.015

APPENDIX A

Deployment Protocol Development for Deriving Accurate Elevational Measurements of a UAS-Based Beach Survey*

Abstract

A methodology is presented for obtaining optimal elevational accuracy using Unmanned Aircraft Systems (UAS) for achieving accurate routine measurements of sand volume changes in beach nourishment projects. Three consumer-grade DJI UAS^{*}, representing a cross-section of capabilities and price ranges, were tested over seventeen flights evaluating UAS elevation and camera pixel resolution, degree of overlap-side lap in taking photos, and number of ground control points (GCP); all with a goal of optimizing flight times to maximize resource conservation. Less than ± 5 cm elevational accuracy was achieved with each system, but with different trade-offs in flight parameters used. The most efficient operational conditions achieved ± 5 cm vertical resolution, while using 40 ground control points, a 20-megapixel camera flown at an elevation of 36m, and 60% overlap, 70% side-lap imaging. Test flights were conducted over a section of a recent beach nourishment in Galveston, Texas.

Introduction

Unmanned Aircraft Systems (UAS) have recently provided a platform to acquire detailed images and other data in sub km² areas while allowing researchers the ability to collect data at their leisure, allowing for long term studies requiring weeks, months, or years of imaging (e.g. Aguilar et al, 2017; Qin et al, 2017, Cook, 2017). The use of UAS presents opportunities to produce high-quality area and volume data as well as other products for GIS as tools for research. As UAS and photogrammetry become more common in research applications a standardized methodology for best use must be established. Using current off-the-shelf consumer-grade UAS, elevation data can be derived to ± 20 cm, research-oriented projects using these systems can achieve ± 10 cm accuracy (e.g. Daponte et al, 2017; Pineux et al, 2017; Weiss and Baret, 2017) with less than ± 5 cm being considered excellent for the purposes of volumetric calculations of features (Day et al, 2016; Boon et al, 2016).

The 2016-2017 “Phase III Beach Nourishment: Seawall East” project on Galveston Island Texas began in December 2016. The nourishment project goal was to replenish and widen the Seawall beach from 10th to 61st streets (6.2km in length and with beaches widened to 91m). The project was completed in May 2017 (Figure 1). This nourishment project presented an opportunity to study the effects of coastal oceanographic and meteorological systems on new beaches over a yearlong study period (e.g. Turner et al, 2016). It was decided to gather data on changes in beach sand volumes on a monthly basis over the length of the project area. UAS-based programmatic survey techniques were chosen to cover the study area in comparison with traditional survey methods for evaluating precision, time and cost effectiveness. Traditional methods of beach survey using RTK systems, total stations, and ground-based LiDAR have been routinely used in monitoring beaches and coastal areas (e.g. Cheng, Wang, Guo, 2016). However, these systems, as well as, aerial-based LiDAR and satellite imaging are oftentimes expensive, labor intensive, or time consuming and therefore not conducted on as frequent a basis as desired for the month-to-month study of the beach nourishment project. UAS models can produce LiDAR-like point clouds generating high resolution topography from low cost UAS (Cook, 2017).

*Reprinted with permission from “Deployment Protocol Development for Deriving Accurate Elevational Measurements of a UAS-Based Beach Survey” by Benjamin Ritt, 2018. Report created for Texas Sea Grant College Program's Grants-In-Aid of Graduate Research Program as part of requirements for grant awardees. Copyright 2018 Benjamin Ritt.

A pre-project imaging phase in December 2016 was conducted and after the nourishment was completed a 12-month monitoring study employing monthly imaging was undertaken to calculate changes in beach volume and profile (e.g. Turner et al, 2016). UAS was decided on as the primary method of gathering data, however to provide useful monitoring of changes in beach volume precise and accurate vertical measurements were required.

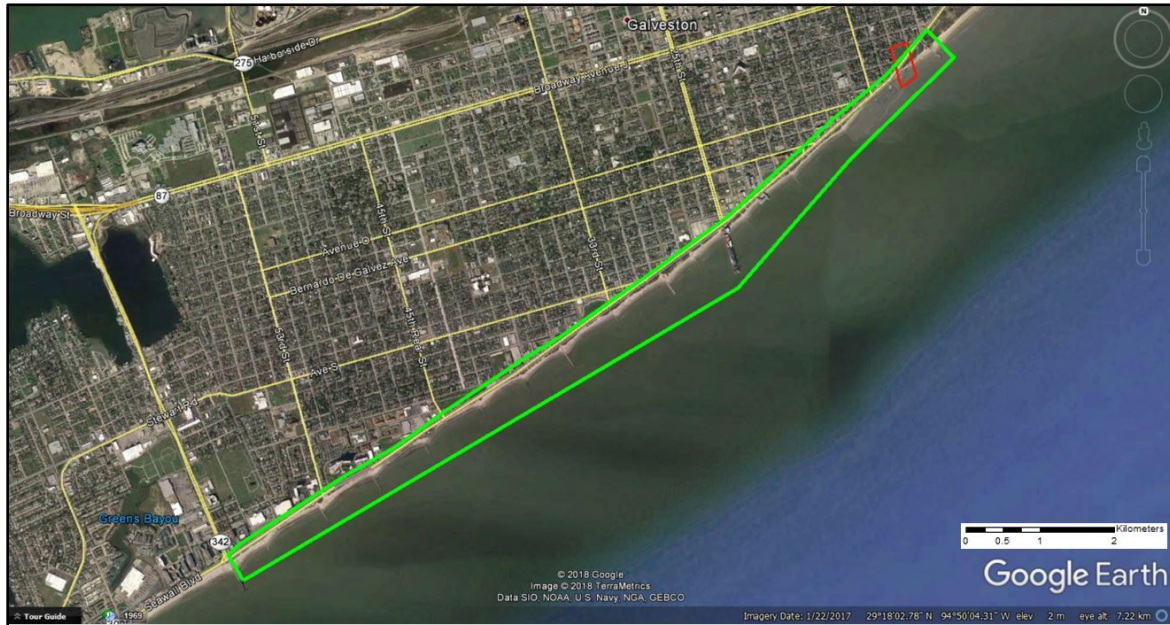


Figure 1 The 2016-2017 Phase III Beach Nourishment: Seawall East project area (green) with Test Area (red). 2 km scale.

Commercial-grade UAS platforms can provide many options in photogrammetric mapping with many of these types of systems providing accurate data through the use of onboard RTK systems, hi-resolution cameras, extended battery life, and control software. However, these systems are usually cost prohibitive for researchers, managing agencies, and organizations looking to gather fast reliable information on coastal systems and projects. A solution is to use a consumer-grade UAS which can be employed as a less expensive option as long as quality assurance steps are taken to gather and create reliable data.

While there are many options in manufacturers and grades of UAS with more becoming available every year, DJI made UAS' were chosen for this project due to their availability, cost, and variety of models. A Phantom 3 Pro, Phantom 4 Pro, and RTK enabled Matrice 600 Pro with 20 Mega Pixel camera were employed for the testing flights (Figure 2). These three UASs provide excellent examples of the different grades of UAS available. The Phantom 3 Pro is equipped with onboard GPS, one Inertial Measurement Unit (IMU) and a 12-mega pixel camera. The Phantom 4 Pro represents the next level of consumer off-the-shelf UAS with improvements in GPS, two IMUs, control hardware, and battery life making it a more advanced option and is equipped with a 20-mega pixel camera. The Matrice 600 Pro represents the high-end range of off-the-shelf UAS or as an entry-level commercial grade unit. This UAS is significantly costlier than the other two platforms but comes with the option to enable it with an onboard RTK system and is capable of carrying multiple imaging payloads. The one used in this testing was equipped with an onboard D-RTK system and a 20-mega pixel camera.

The project utilized Agisoft PhotoScan Pro to process images into point clouds, 3D meshes, orthomosaics, and Digital Elevation Models (DEMs). The successful photogrammetry using structure in motion software requires the images being used to have an overlap and side-lap of at least 50% and be

taken as uniformly as possible (Kraus, 2007; Ibraheem, Daham, Hussein, 2014). We used DroneDeploy, a flight planning software tool to select image overlap and side-lap from 50/50 to 95/95, and altitude to be adjusted for a range of pixel resolutions to capture detail of the mapped surface. Good resolution in imaging and thusly the models, DEMs, and orthomosaics is essential for ensuring that the locating and marking of features as well as measurements are as accurate as possible. These settings affect the number of flights required to complete imaging of the test area with lower altitude flights with greater overlap and side-lap require a larger investment in time and resources like batteries and data storage for the increased number of images taken. A compromise in the ratio of images gathered at the highest resolution (i.e. flight altitude) and flight time was established. A testing protocol to determine this ratio was established where images would be taken using the three different DJI UAS platforms in a range of altitudes and overlap and side-lap options from 50/50 at 25m to 70/70 at 61m. While the three UASs were tested, a DJI Phantom 4 Pro was chosen for the majority of testing flights with the other two, a DJI Phantom 3 Pro and an RTK-enabled DJI Matrice 600 Pro being used to test the effectiveness of what was determined to be the best overlap and side-lap to altitude ratio across a less expensive and more expensive platform (figure 2).




		
<p><u>Phantom 3 Pro</u></p>	<p><u>Phantom 4 Pro</u></p>	<p><u>Matrice 600 Pro</u></p>
<ul style="list-style-type: none"> • 12MP Camera • 15-20 Minute flight time • 1 Onboard GPS/GLONASS • Onboard compass • 1 IMU • 1280g with Battery • \$800 US • Elevation error for 1 GCP is +/- 38 cm 	<ul style="list-style-type: none"> • 20MP Camera • 25-30 Minute flight time • 1 Onboard GPS/GLONASS • Dual onboard compass • 2 IMU • 1388g with battery • \$1400 US • Elevation error for 1 GCP is +/- 28 cm 	<ul style="list-style-type: none"> • 20MP Camera used compatible with other camera systems. • Can carry a 5.8kg payload • 45 Minute-1 hour flight time • Requires 6 batteries to fly • 3 Onboard GPS/GLONASS receivers. • 3 IMU • RTK compatible • 9.1 kg with batteries • \$10,000 US – with RTK • Elevation for 1 GCP is +/- 22 cm

Figure 24 DJI made UAS models used for the testing at the 3.23-hectare testing area.

Methods

Seventeen flights were conducted, with thirteen flown using the Phantom 4 Pro. The remaining flights were divided between the Phantom 3 Pro and Matrice 600 Pro once the best overlap, side-lap, and altitude ratios had been identified to determine if that ratio was effective across all platforms.

A 3.23 hectares test area was chosen inside the Phase III Beach Nourishment: Seawall East project area between two groins (Figure 3). This location was chosen because of it had open field areas that could be used to increase the measurable space north of the Seawall, its relatively close proximity to the RTK monument, and for its lack of popularity as a tourist spot thus limiting interference in data collection.

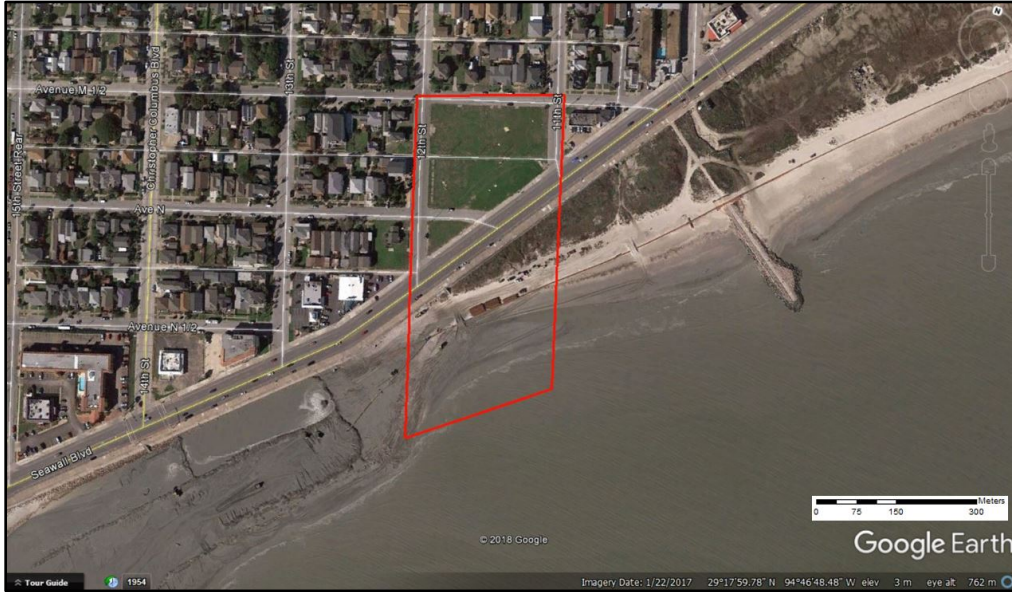


Figure 3 The 3.23-hectare testing area used for testing flights using the Phantom 3 Pro, Phantom 4 Pro, and Matrice 600. Pro.

Weather and sun angle were important factors that were taken into consideration for these tests and in the planning of the beach nourishment monitoring project. Wind is obviously a limiting factor to flight times as fighting against wind drains batteries faster than in calm conditions. Cloud cover and low sun angles can create spots where low light conditions and long shadows appear in the imagery. Programmatic software will sometimes interpret these features as negative spaces, unintentionally adding depth to a surface. To mitigate these effects both protocol development and surveying flights were planned for days with minimal wind and cloud cover and planned around sun angles greater than 40 degrees above the horizon, in addition, flights were flown during low tide to maximize beach exposure.

The thirteen testing flights conducted with the Phantom 4 Pro were planned using DroneDeploy software so that flight parameters could be closely controlled and data on flight times and resolution would be recorded. These thirteen flights were designed to cover the range of variable overlap, side-lap, and altitude ratios in image capturing for processing in Agisoft Photoscan Pro to determine which ratio presented the best resolution in ortho imagery, accuracy in elevation measurements, and most efficient time and resource allocation per flight. In-field processing of the images on a mobile workstation laptop allowed the Phantom 3 Pro and Matrice 600 Pro flights to be planned and executed to test if the optimal altitude and overlap and side-lap determined for the Phantom 4 Pro would work for those other platforms as well. In total seventeen flights were made for the field-testing phase of this project.

Flight altitudes (25m, 36m, 48m, and 61m) were chosen for the test flights to represent a range of viable altitudes that guaranteed that the UAS would safely clear ground obstacles and not exceed a resolution of 2.0 cm/pix which altitudes over 61m generated. It was surmised that pixel resolution was

also an indicator of elevational measurement accuracy. Excellent pixel resolution aided in the accurate placement of GCPs in the models. Ratios of overlap and side-lap were chosen to represent a range from the minimum required for the programmatic process to work (50/50) and what was determined to be a maximum of 70/70 as ratios over this increased flight times past an acceptable limit. In addition, a 60/70 ratio was added to determine if this was the optimal ratio for UAS based photogrammetric surveying per one of the DroneDeploy software defaults.

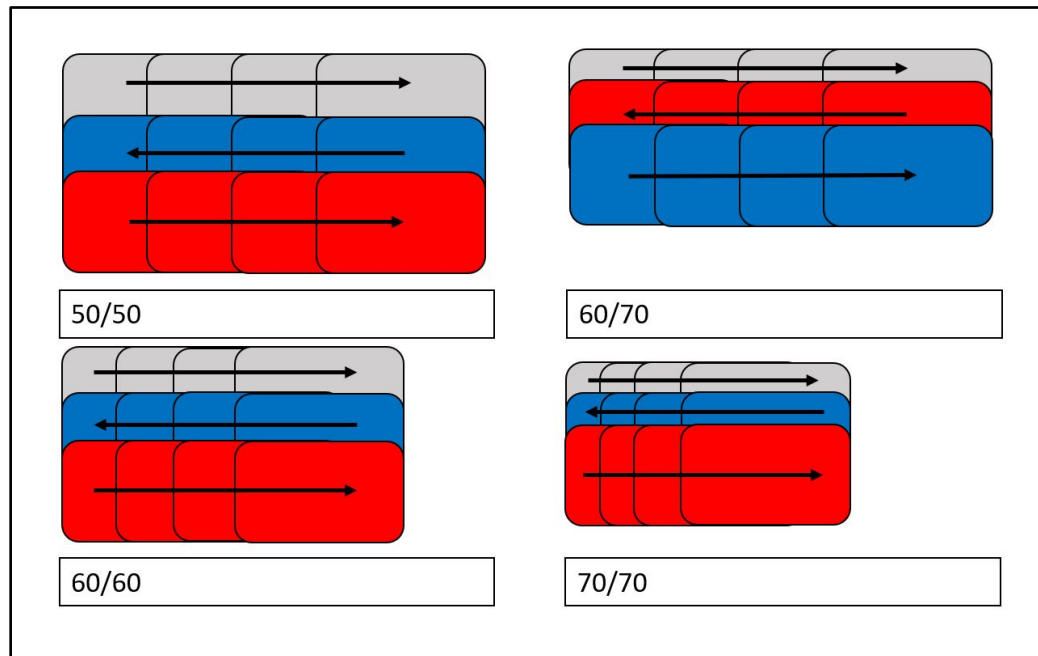


Figure 4 Examples of the difference in camera overlap and side-lap used.

Once flight planning was completed, testing with the three UAS platforms was conducted at the test area. In order to geo-reference the produced programmatic models and products, 40 GCPs were placed across the test area. These consisted of thirty-six 26cm² coded targets (Figure 6) created by Agisoft Photoscan Pro affixed to 0.914m long scale bars with the remaining 4 GCPs being chosen from easily recognized points in the hard structure of Galveston's Seawall. The use of the 0.914m scale bars with coded targets attached was chosen to ensure that GCP targets would be evenly placed and allowed for a quality control measurement in the models produced. If the measurement between coded targets were much greater or smaller (+/- 2cm) than the 0.914m known length of the scale bar steps were taken to correct the underlying issue that caused this error ensuring the greatest possible accuracy in measurements. All points were measured using a Leica Viva GS10 RTK system monumented to a National Geodetic Survey Benchmark for GPS and Vertical control set in the top of the Seawall. Geo-referencing the models produced in Photoscan Pro using RTK derived GCPs ensures the produced data is accurate and allows for the creation of accurate DEMs for use in profile and volumetric calculations (Ruzgienė et al, 2015). Coded target GCPs offer the ability to place GCPs on any surface being surveyed and have Photoscan Pro detect the targets in the imagery taken. GCPs can also be created using points on hard structures that are easily identifiable.

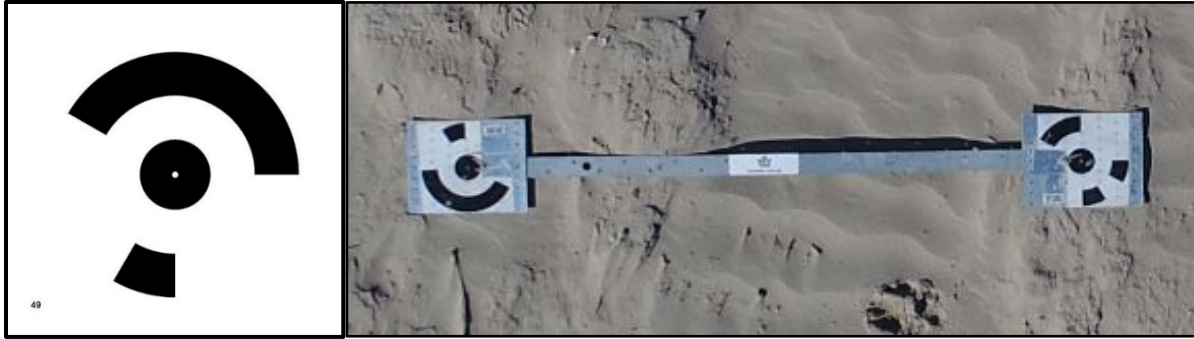


Figure 5 Examples of Agisoft Photoscan coded target pattern and pattern printed out in 26cm² used for ground control points Attached to the 0.914 m long scale bars for quality assurance in measurements.



Figure 6 Orthomosaic showing the placement of the 40 Ground Control Points for the 3.23-hectare test area.

The use of forty GCPs and their distribution across the test area was decided for georeferencing the models and to provide several layers of redundant quality assurance measurements in evaluating the final accuracy of the models and products produced (Casella et al, 2014; Agüera-Vega, Carvajal-Ramírez, Martínez-Carricondo, 2017). This was accomplished by comparing the original RTK elevation measurement for each point and the estimated elevation produced by Agisoft Photoscan Pro By placing the GCP scale bars in a pattern that runs parallel to the seawall and perpendicular to each other along the beach allowed for the testing of the number of required GCPs as well as reference quality. This GCP

placement method also allowed for the creation of an RTK point based profile for quality assurance testing of the models and DEMs produced.

Flights conducted with the RTK enabled Matrice 600 Pro were conducted last so that the base station for the RTK could be monumented the same way the Leica Viva GS10 base station was. This was done using a tripod system, laser tape measure, and the National Geodetic Survey Benchmark information being entered into the RTK control suite in the DJI Assistant 2 software used to interface with the UAS. This UAS system allowed for a rapid deployment and gathering of quality georeferenced images using the RTK mounted on the UAS (Turner, Harley, Drummond, 2016). Images gathered these flights were processed exactly the same as the other images taken with other platforms however, the GCP targets were used as check points where the difference between the known handled RTK elevational data and the UAS RTK elevational data would be deducted from each other to determine the elevational error in the models and DEMs.

Post processing of the seventeen image sets from the flights was conducted over the next week following the general work flow provided by Agisoft Photoscan Pro and the basic process for adding ground control points to the dense clouds and meshes produced to geo-reference the finished products. In addition to these models, two additional models were produced from the most promising data set to test if the number and density of deployed GCPs resulted in more accurate elevational measurements (James et al, 2017). To ensure that our methods would yield the best results a test was devised to determine the limiting factor of the number of used GCPs. After postprocessing of the images for each flight was completed the data set with the best results was taken and the used GCPs were reduced by half for each iteration of the model produced until only 1 GCP was being used (Figure 8).

P4 60/70 36m # GCPs	40	20	10	5	1
DEM cm/pix	1.94	1.94	1.94	1.94	1.94
Ortho cm/pix	0.97	0.97	0.97	0.97	0.97
GCP elevation error in cm	3.06	6.89	9.40	23.56	28.12

Table 1 Results of GCP quantities test for using the Phantom 4 Pro over the 3.23-hectare Test Area.

Results

Analysis of the post processing data from Agisoft Photoscan Pro for the thirteen testing flights with the Phantom 4 Pro produced a range of data (Figures 9&10) that was used to help determine which altitude and overlap to side-lap ration produced the best accuracy in elevational measurements for volumetric calculations of sand while being the most time and resource efficient. Elevational errors were calculated by deducting values from the DEM value at the same point as GCPs by drawing a point on the GCP in the DEM and measuring its position and elevation (Uysal et al, 2015).

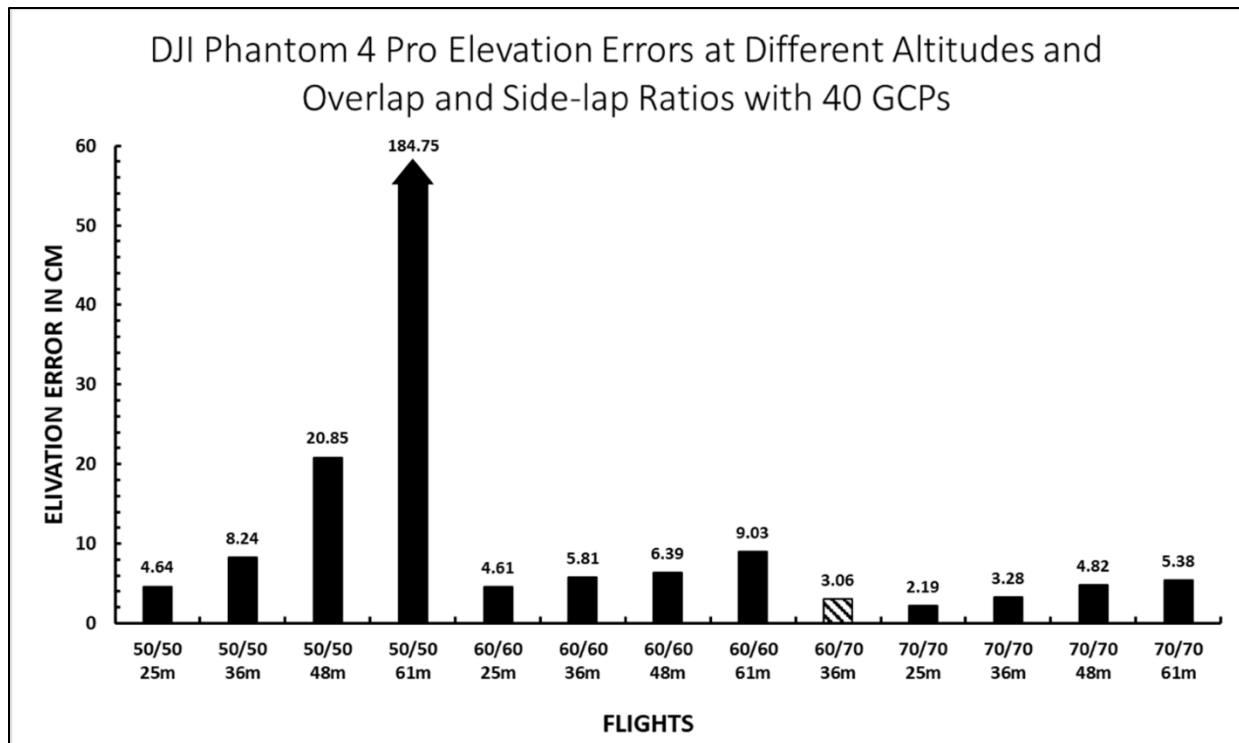


Figure 25: Elevation error data in centimeters for 13 flights using the Phantom 4 Pro over the 3.23-hectare test area using 40 GCPs.

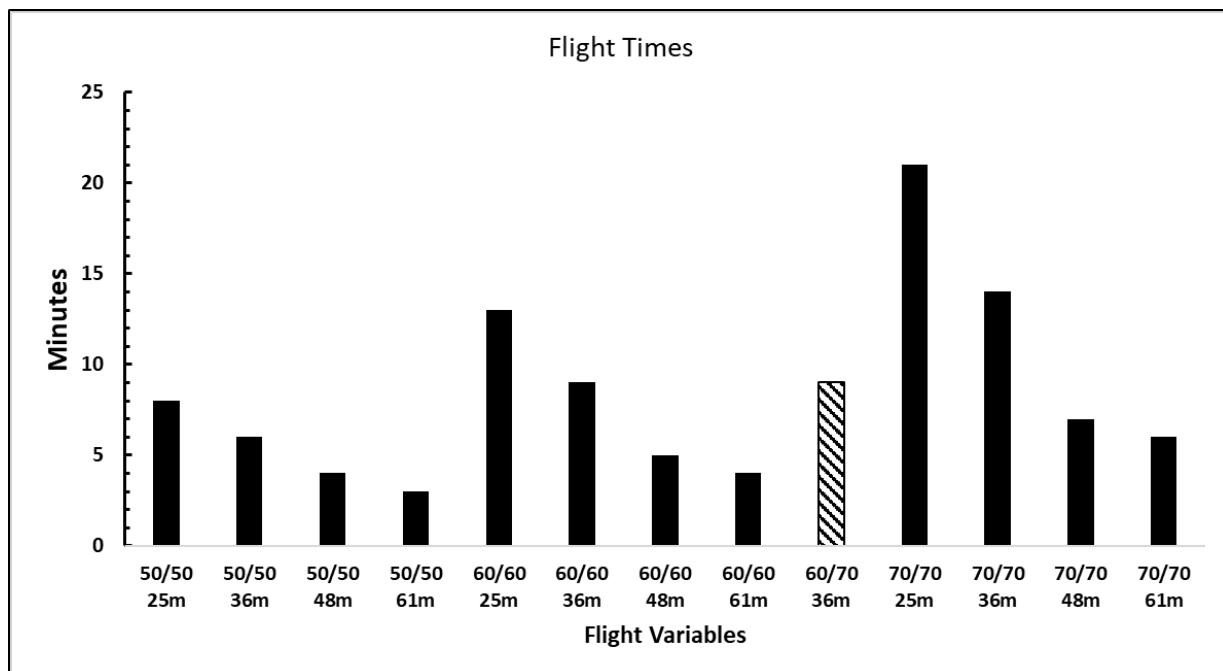


Figure 8: Flight time data for 13 flights using the Phantom 4 Pro over the 3.23-hectare test area.

While 70/70 overlap produced the smallest error when flown from an altitude of 25m (2.2cm) the amount of flight time to cover the test area was excessive. With this altitude 21:18 minutes for 3.23

hectares was multiplied to account for the entire area of the beach nourishment study area with its 121.40 plus hectares area an approximate need flight time of 787 minutes (13hrs) was calculated to complete the study. Using the recommended Drone Deploy settings of 60 /70 at an altitude of 36m produced the next smallest error in elevational measurements (3.1cm) and with a significantly reduced flight time at 8:52 minutes required to cover the test area and the subsequently the beach nourishment study area with a calculated required flight time of 337 minutes (5.5hrs). Since the objective of the beach nourishment study is to complete monthly surveys in as little time as possible while retaining the highest accuracy in elevational measurements the 60/70 overlap/side-lap at 36m altitude was decided upon.

It is however important to note that other ratios of overlap and side-lap produced sub 5cm elevation errors (50/50 36m, 60/60 36m, 70/70 36m, 70/70 48m) with all but 70/70 36m staying under a 10-minute flight time. This would make these other ratios useful for projects whose scope does not require the highest degree of elevation accuracy desired for this study. In addition, tests of the number of GCPs used 40, 20,10, & 1 (Figure 7) showed that even the use of 20 or 10 GCPs using the 60/70 ratio at 36m produced sub +/- 10cm elevation errors.

Discussion

Data sets for the Phantom 3 Pro using this protocol produced elevational errors of 8.0 cm at 36m and the 2.2cm at 36m with the RTK enabled Matrice 600 Pro UAS. While results with the Phantom 3 Pro were not as desirable as the Phantom 4 Pro or the Matrice 600 Pro they fall below the 10cm mark. The Phantom 3 Pro was used in these tests to represent the low end of the consumer UAS available which can still be used for studies like the one being conducted in Galveston. The RTK enabled Matrice 600 Pro Produced the best(smallest) elevational errors due to its precision guidance, and the ability to accurately geotag images using RTK-derived geodetic data.

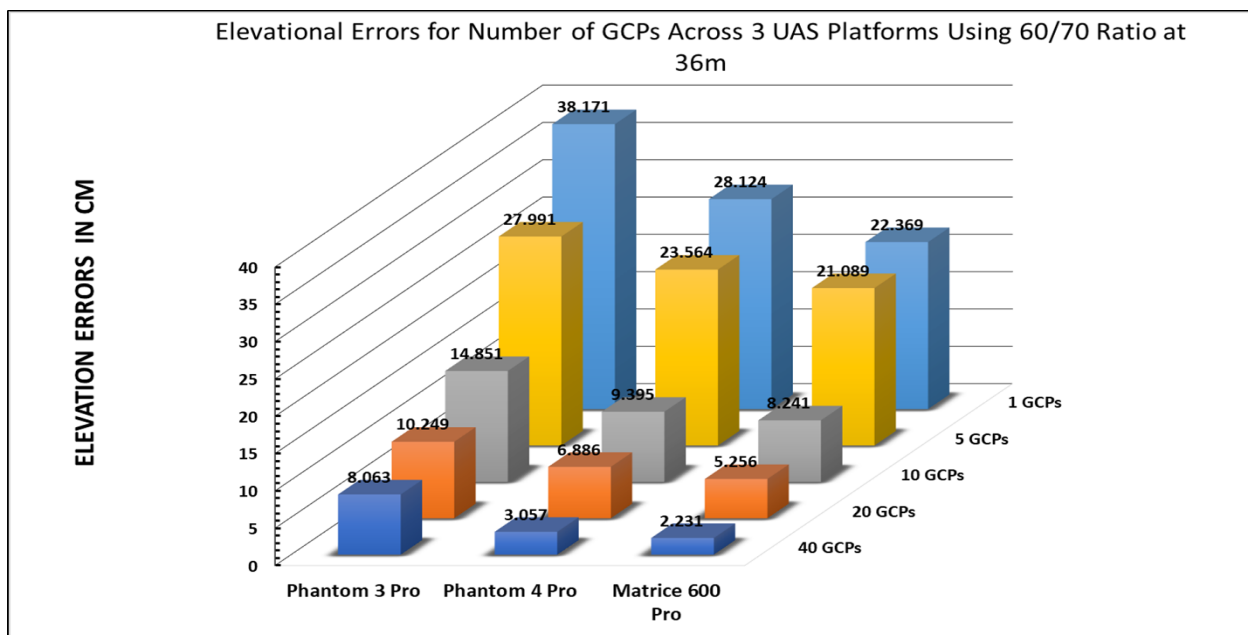


Figure 9 Comparison of elevational errors between Phantom 3 Pro, Phantom 4 Pro, & Matrice 600 Pro at 60 /70 overlap at 36m

The protocol for 60/70 ratio at an altitude of 36m established by this testing has proven effective at deriving accurate volumetric calculations in photogrammetric surveying through its accuracy in elevational measurements. Such accuracy is essential in producing high quality data sets for use by

researchers, managing agencies, and local organizations using UAS based photogrammetric methods for coastal projects.

Practical applications

Using the 60/70 ratio at an altitude of 36m and the forty GCP method monthly flights were planned to start capturing the beach nourishment study area which had been broken up into five sections. Currently ten months of UAS based imagery for photogrammetric surveying has been conducted of the study area using this protocol. After the images are processed orthomosaics and DEMs are created in Agisoft Photoscan Pro. Using DEMs with contour lines from the December 2016 pre-nourishment survey flights the areas where sand was added and where dunes and vegetation were avoided can be delineate. Polygons are then drawn to make volume calculations of beach sand for each section using Photoscan Pro's in-house volumetric calculation tool set to a custom base plane of mean sea level recorded by a NOAA Station at the Galveston Bay Entrance, for the time period that the imagery was taken.

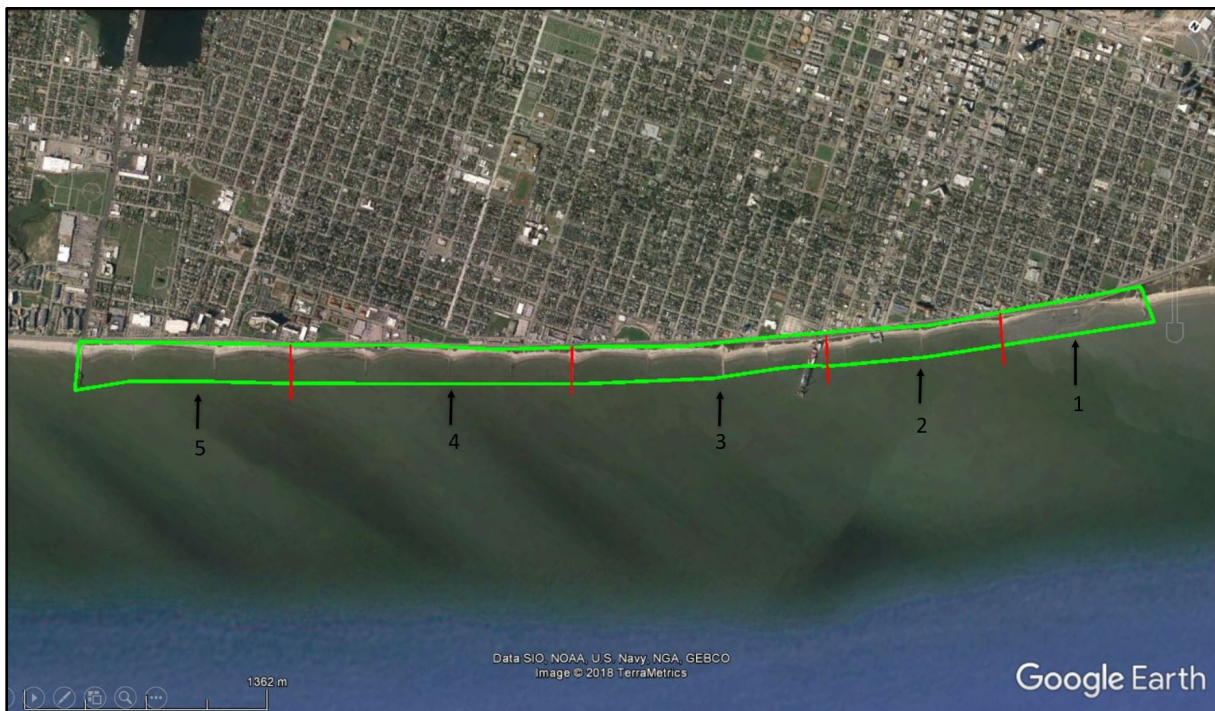


Figure 10 The five sections of the Beach nourishment monitoring study area.

Twelvemonths of data have been collected with this initial monitoring study (Ritt and Jones, in prep). Using the methodology established in this paper; models, DEMs, and other products were produced for Section 1 which represents the longest distance between any two groins (850m) in the beach nourishment area along the Galveston seawall as an example for this paper. Forty GCPs were chosen along the Seawall's hard structure and that of the groins that bookend the section. The placement of the GCPs as such allows for their reuse for every survey of that section reducing required field time and simplifying the process (Casella et al, 2014). Two scale bars with coded targets (Figure 6) were placed in the middle of the section for quality assurance measurements as well.



Figure 26 Section1 of the Beach Nourishment study area with distribution of GCPs and scale bars and the location of the profile taken in the center (red).

Each flight of this section took approximately 40 minutes and 30 seconds and required 3 batteries to complete using the 60/70 ratio for 18-hectare flight area. Post processing of the images for this section were completed for the ten months of the study as it has been conducted so far. Once DEMs were created for each month profiles and volumes were calculated in order to track change in the section. A polyline was drawn in each section from the base of the seawall to the water line. The location along the seawall for this polyline placement was chosen to be in line with a National Geodetic Survey bench mark AW0588 and for its location near to center of the section.

The above the waterline volumetric measurements of beach sand in the section allowed for the creation of a trend model that depicts the average loss of sand for the beach section over a 10-month period. This volume trend showed that after an initial high-volume loss in the first 2 months directly after the nourishment project concluded the beach maintained a much smaller steadier rate of sand loss. The initial loss during the first 2 months is most likely due to the formation of a more natural beach profile from that which was created during the process of adding the sand (Figure 15).

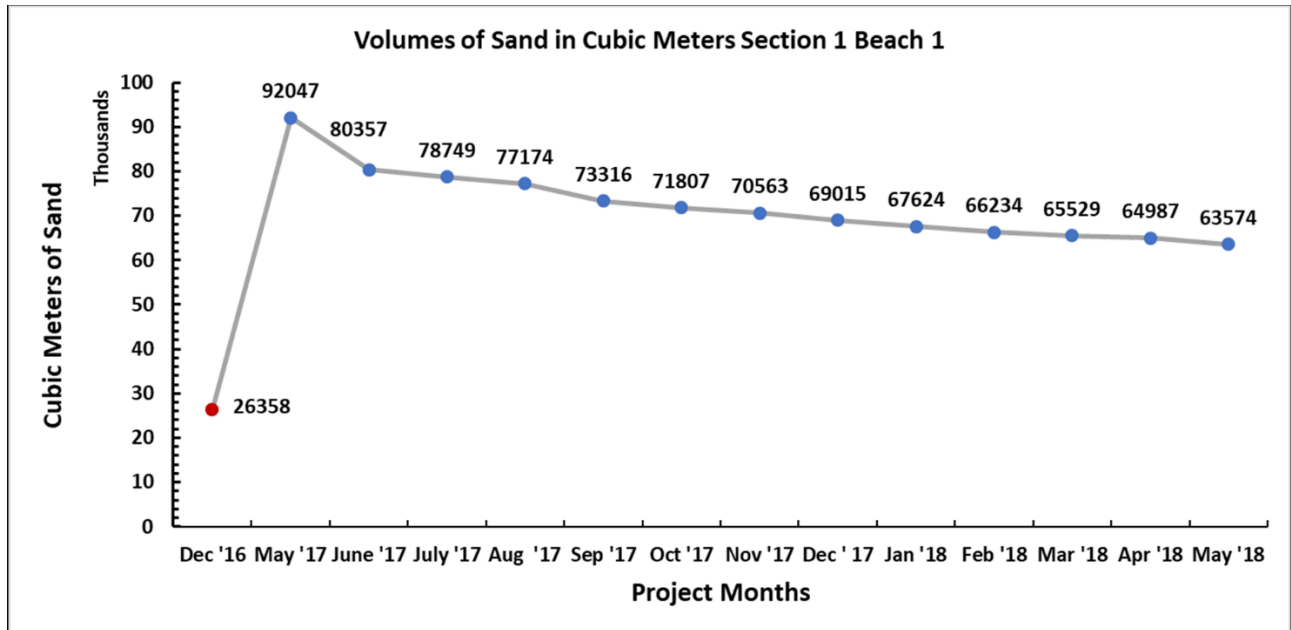


Figure 27 Volume calculations of Beach sand for Section 1 Beach 1 of the Beach Nourishment monitoring project.

In addition to volume calculations a profile was created for each month (Figure 14) from the middle of the section (Figure 12) to help better explain the nature of the change to the newly nourished beach and to see if the profile would help explain the trends in sand volume loss from above the waterline. These profiles show the change that the beach has experienced over the last ten months of the study. Of particular note is the shape of the beach in May 2017 and June 2017 right after the nourishment project was completed. These profiles show how the addition of sand during the nourishment created a beach surface that had a flat structure with a lip close to 40 meters from the seawall. This structure was created during nourishment to help retain sand during beach building and its erosion along with the grading of the beach through natural processes helps explain the high amount of loss in the initial 2 months after the nourishment was finished. After that time the beach more gradually hit a point of homeostasis and volume loss decreased with time.

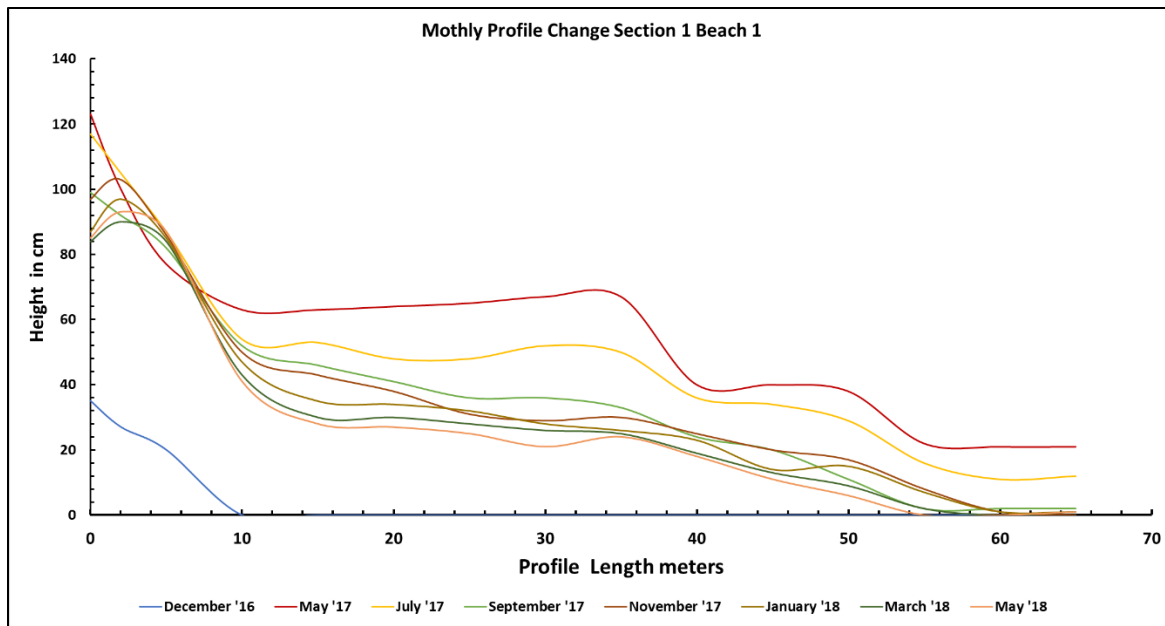


Figure 29 Alternating Monthly Beach Profiles for Section 1 Beach 1

Definitions

DEM- Digital Elevation Model

RTK- Real Time Kinetics

GPS- Global Positioning System

IMU- inertial measurement unit

UAS- Unmanned Aircraft System was adopted as the official terminology by the United States Department of Defense (DoD) and the United States Federal Aviation Administration in 2005 according to their Unmanned Aircraft System Roadmap 2005–2030.

UAV- Unmanned Aerial Vehicle as a term has been adopted by many other nations airspace control agencies and can be used interchangeably with UAS.

GCP- Ground Control Point

DJI- Dà-Jiāng Innovations Science and Technology Co., Ltd

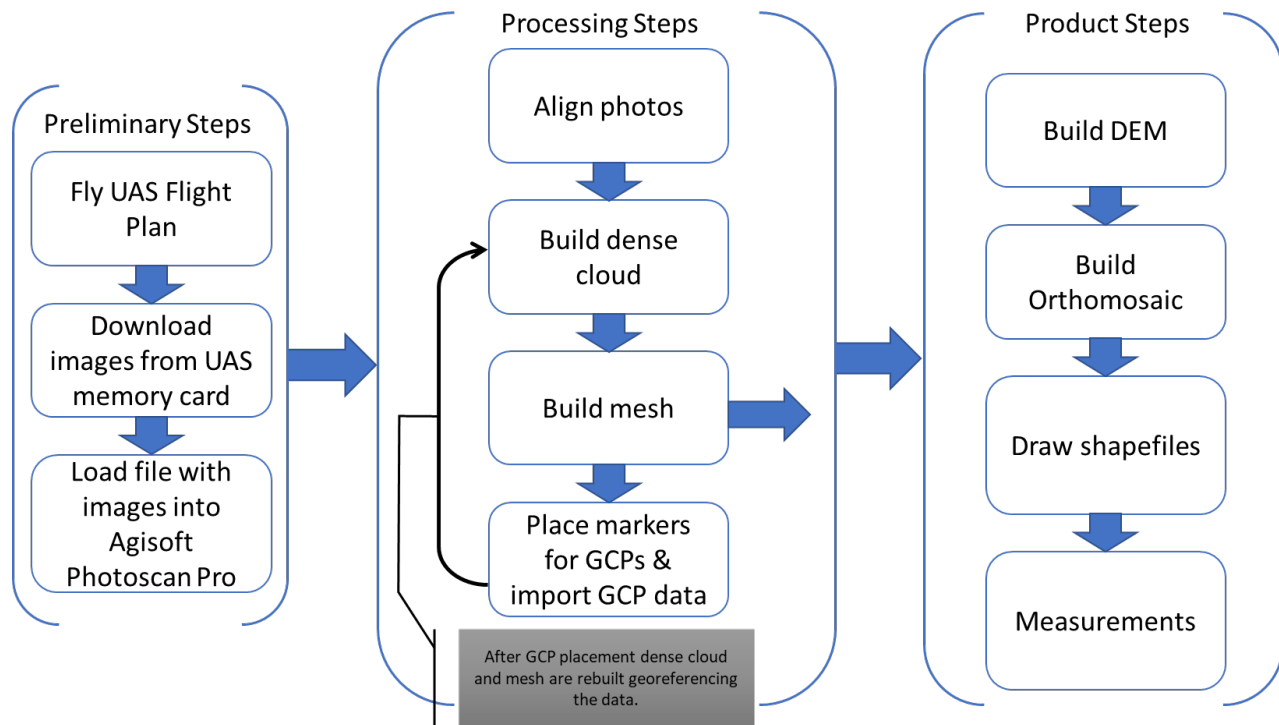
Literature Cited

- Aguilar, F. J., Fernandez, I., Casanova, J. A., Manuel, M. A., & Blanco, J. L. (2016). Advances on Mechanics, Design Engineering and Manufacturing (pp. 879-887). Catania, Italy: *Springer*. Retrieved from https://link.springer.com/chapter/10.1007_2F978-3-319-45781-9_88
- Agüera-Vega, F., Carvajal-Ramírez, F., & Martínez-Carricondo, P. (2017). Assessment of Photogrammetric mapping accuracy based on variation ground control points number using unmanned aerial vehicle. *Measurement*, 98, 221-227. doi:10.1016/j.measurement.2016.12.002
- Boon, M. A., Greenfield, R., & Tesfamichael, S. (2016, September). Unmanned Aerial Vehicle (UAV) Photogrammetry Produces Accurate High-resolution Orthophotos, Point Clouds and Surface Models for Mapping Wetlands. *South African Journal of Geomatics*, 5(2). doi:10.4314/sajg.v5i1.187
- Casella, E., Rovere, A., Pedroncini, A., Mucerino, L., Casella, M., Cusati, L. A., Firpo, M. (2014). Study of wave runup using numerical models and low-altitude aerial photogrammetry: A tool for coastal management. *Estuarine, Coastal and Shelf Science*, 149, 160-167. doi:10.1016/j.ecss.2014.08.012
- Cheng, J., Wang, P., & Guo, Q. (2016). Measuring Beach Profiles along a Low-Wave Energy Microtidal Coast, West-Central Florida, USA. *Geosciences*, 6(4), 44. doi:10.3390/geosciences6040044
- Cook, K. L. (2017). An evaluation of the effectiveness of low-cost UAVs and structure from motion for geomorphic change detection. *Geomorphology*, 278, 195-208. doi:10.1016/j.geomorph.2016.11.009
- Daponte, P., De Vito, L., Mazzilli, G., Picariello, F., & Rapuano, S. (2017, February). A height measurement uncertainty model for archaeological surveys by aerial photogrammetry. *Measurement*, 98, 192-198.
- Day, D., Weaver, W., & Wilsing, L. (2016, December). Accuracy of UAS Photogrammetry: A Comparative Evaluation [Electronic version]. *Photogrammetric Engineering & Remote Sensing*, 82(12), 909-914.
- Ibraheem, A. T., Daham, A. M., & Hussein, S. N. (2014). Coupling GIS and Photogrammetry for the Development of Large-Scale Land Information System (LIS). *Journal of Geosciences and Geomatics*, 2(1), 1-10. doi:DOI: 10.12691/jgg-2-1-1
- Kraus, K. (2007). Photogrammetry geometry from images and laser scans. Berlin: Walter De Gruyter.
- Pineux, N., Lisein, J., Swerts, G., Bièlders, C. L., Lejeune, P., Colinet, G., & Degré, A. (2017, March). Can DEM time series produced by UAV be used to quantify diffuse erosion in an agricultural watershed? *Geomorphology*, 280, 122-136. doi:http://doi.org/10.1016/j.geomorph.2016.12.003
- Qin, R., Tian, J., & Reinartz, P. (2016, December). 3D change detection – Approaches and applications [Electronic version]. *ISPRS Journal of Photogrammetry and Remote Sensing*, 122, 41-56.
- Ruzgienė, B., Berteška, T., Gečyte, S., Jakubauskienė, E., & Aksamitauskas, V. Č. (2015). The surface

- modelling based on UAV Photogrammetry and qualitative estimation. *Measurement*, 73, 619-627. doi:10.1016/j.measurement.2015.04.018
- Turner, I. L., Harley, M. D., & Drummond, C. D. (2016). UAVs for coastal surveying. *Coastal Engineering*, 114, 19-24. doi:10.1016/j.coastaleng.2016.03.011
- Turner, I. L., Harley, M. D., Short, A. D., Simmons, J. A., Bracs, M. A., Phillips, M. S., & Splinter, K. D. (2016). A multi-decade dataset of monthly beach profile surveys and inshore wave forcing at Narrabeen, Australia. *Scientific Data* ,3, 160024. doi:10.1038/sdata.2016.24
- Uysal, M., Toprak, A., & Polat, N. (2015). DEM generation with UAV Photogrammetry and accuracy analysis in Sahitler hill. *Measurement*, 73, 539-543. doi:10.1016/j.measurement.2015.06.010
- Weiss, M., & Baret, F. (2017, January 28). Using 3D Point Clouds Derived from UAV RGB Imagery to Describe Vineyard 3DMacro-Structure. *Remote Sensing*, 9(2). doi:10.3390/rs9020111

APPENDIX B

Agisoft Photoscan Pro workflow used to process images to finished models, DEMs, and orthomosaics for measurements.



APPENDIX C

RTK and UAS Profile Longitude, Latitude, and Altitude data.

(EPSG:32615 WGS 84 / UTM zone 15N); Profile Length & Z/Altitude measurements in meters

Profile Length	RTK X/Longitude	RTK Y/Latitude	RTK Z/Altitude	UAS X/Longitude	UAS Y/Latitude	UAS Z/Altitude
0	-94.783887	29.293142	1.487000	-94.78388697	29.29314152	1.49
1	-94.783880	29.293134	1.451000	-94.78388049	29.29313426	1.452
2	-94.783874	29.293128	1.436000	-94.78387438	29.29312796	1.43
3	-94.783868	29.293122	1.424000	-94.78386826	29.29312196	1.42
4.7	-94.783859	29.293111	1.215000	-94.78385854	29.29311124	1.22
5	-94.783854	29.293106	1.138000	-94.78385387	29.29310619	1.13
6	-94.783847	29.293100	1.135000	-94.78384739	29.29309989	1.127
7	-94.783841	29.293092	1.124000	-94.78384091	29.29309232	1.125
8	-94.783835	29.293086	1.119000	-94.7838348	29.29308601	1.116
9	-94.783828	29.293079	1.111000	-94.78382832	29.29307875	1.114
10	-94.783823	29.293073	0.982000	-94.78382257	29.29307276	0.99
11	-94.783817	29.293067	0.919000	-94.78381681	29.29306677	0.92
12	-94.783812	29.293062	0.887000	-94.78381177	29.29306172	0.877
13	-94.783807	29.293057	0.864000	-94.78380709	29.29305699	0.863
14	-94.783802	29.293051	0.855000	-94.78380206	29.293051	0.859
15	-94.783787	29.293035	0.723000	-94.78378659	29.29303491	0.71
16	-94.783781	29.293029	0.710000	-94.78378119	29.29302924	0.702
17	-94.783776	29.293024	0.698000	-94.78377579	29.29302356	0.69
18	-94.783770	29.293017	0.674000	-94.78377005	29.29301732	0.681
19	-94.783764	29.293011	0.651000	-94.78376429	29.29301133	0.666
20	-94.783759	29.293005	0.641000	-94.78375853	29.29300471	0.64
21	-94.783752	29.292999	0.629000	-94.78375242	29.29299871	0.613
21	-94.783745	29.292991	0.611000	-94.78374486	29.29299083	0.608
23	-94.783739	29.292984	0.603000	-94.78373874	29.2929842	0.601
24	-94.783733	29.292977	0.594000	-94.78373263	29.29297663	0.588
25	-94.783724	29.292968	0.581000	-94.78372399	29.29296812	0.574
26	-94.783716	29.292960	0.577000	-94.78371608	29.29296023	0.57
27	-94.783707	29.292950	0.575000	-94.78370708	29.29295014	0.568
28	-94.783700	29.292943	0.573000	-94.78369989	29.29294257	0.568
29	-94.783692	29.292934	0.564000	-94.78369161	29.29293406	0.566
30	-94.783686	29.292927	0.561000	-94.78368621	29.29292743	0.564
31	-94.783677	29.292918	0.559000	-94.7836765	29.29291766	0.56
32	-94.783669	29.292911	0.553000	-94.7836693	29.29291072	0.55
33	-94.783661	29.292902	0.553000	-94.78366139	29.29290189	0.554
34	-94.783655	29.292895	0.551000	-94.78365543	29.29289524	0.55
Profile Length	RTK X/Longitude	RTK Y/Latitude	RTK Z/Altitude	UAS X/Longitude	UAS Y/Latitude	UAS Z/Altitude

35	-94.783639	29.292878	0.549000	-94.78363929	29.29287837	0.55
36	-94.783634	29.292872	0.520000	-94.78363363	29.29287216	0.534
37	-94.783626	29.292864	0.508000	-94.78362599	29.29286373	0.512
38	-94.783618	29.292857	0.489000	-94.78361834	29.29285653	0.497
39	-94.783613	29.292851	0.465000	-94.78361325	29.29285082	0.476
40	-94.783606	29.292843	0.455000	-94.78360645	29.29284338	0.46
41	-94.783602	29.292839	0.426000	-94.78360221	29.29283891	0.444
42	-94.783597	29.292834	0.419000	-94.7835974	29.29283444	0.431
43	-94.783592	29.292828	0.412000	-94.7835923	29.29282849	0.42
44	-94.783587	29.292822	0.397000	-94.78358692	29.29282179	0.406
45	-94.783580	29.292814	0.374000	-94.78357956	29.29281434	0.39
46	-94.783574	29.292809	0.356000	-94.7835739	29.29280863	0.376
46	-94.783569	29.292803	0.338000	-94.78356852	29.29280268	0.34
48	-94.783565	29.292799	0.302000	-94.78356484	29.2927992	0.3
49	-94.783560	29.292795	0.263000	-94.78356031	29.29279474	0.274
50	-94.783555	29.292790	0.284000	-94.78355522	29.29278953	0.29
51	-94.783550	29.292783	0.254000	-94.7835504	29.29278307	0.248
52	-94.783545	29.292778	0.198000	-94.78354499	29.29277758	0.185
53	-94.783540	29.292773	0.157000	-94.78354043	29.29277266	0.164
54	-94.783534	29.292766	0.142000	-94.78353377	29.2927659	0.133
55	-94.783527	29.292759	0.123000	-94.78352728	29.29275883	0.11
56	-94.783520	29.292751	0.009000	-94.78351992	29.29275115	0.006
56	-94.783512	29.292743	0.007000	-94.78351239	29.29274301	0.005
58	-94.783504	29.292734	0.004000	-94.78350415	29.2927341	0.003
59	-94.783497	29.292726	0.004000	-94.78349679	29.29272642	0.001